Monthly Notices of the ROYAL ASTRONOMICAL SOCIETY

Mon. Not. R. Astron. Soc. **417,** 2831–2845 (2011) doi:10.1111/j.1365-2966.2011.19445.x

ACCESS – IV. The quenching of star formation in a cluster population of dusty S0s

C. P. Haines,[1,2]★ P. Merluzzi,[3] G. Busarello,[3] M. A. Dopita,[4,5,6] G. P. Smith,[2] F. La Barbera,[3] A. Gargiulo,[7] S. Raychaudhury[2] and R. J. Smith[8]

[1] *Steward Observatory, University of Arizona, 933 North Cherry Avenue, Tucson, AZ 85721, USA*
[2] *School of Physics and Astronomy, University of Birmingham, Edgbaston, Birmingham B15 2TT*
[3] *INAF – Osservatorio Astronomico di Capodimonte, via Moiariello 16, I-80131 Napoli, Italy*
[4] *Research School of Astronomy and Astrophysics, Australian National University, Cotter Road, Weston Creek, ACT 2611, Australia*
[5] *Astronomy Department, King Abdulaziz University, PO Box 80203, Jeddah, Saudi Arabia*
[6] *Institute for Astronomy, University of Hawaii, 2680 Woodlawn Drive, Honolulu, HI 96822, USA*
[7] *INAF – Osservatorio Astronomico di Brera, via Brera 28, I-20121 Milano, Italy*
[8] *Department of Physics, University of Durham, Durham DH1 3LE*

Accepted 2011 July 13. Received 2011 July 12; in original form 2011 May 6

ABSTRACT

We present an analysis of the mid-infrared (MIR) colours of 165 70-μm-detected galaxies in the Shapley supercluster core (SSC) at $z = 0.048$ using panoramic *Spitzer*/MIPS 24- and 70-μm imaging. While the bulk of galaxies show f_{70}/f_{24} colours typical of local star-forming galaxies, we identify a significant subpopulation of 23 70-μm-excess galaxies, whose MIR colours ($f_{70}/f_{24} > 25$) are much redder and cannot be reproduced by any of the standard model IR spectral energy distributions (SEDs). These galaxies are found to be strongly concentrated towards the cores of the five clusters that make up the SSC, and also appear rare among local field galaxies, confirming them as a cluster-specific phenomenon. Their optical spectra and lack of significant ultraviolet emission imply little or no ongoing star formation, while fits to their panchromatic SEDs require the far-IR emission to come mostly from a diffuse dust component heated by the general interstellar radiation field rather than ongoing star formation. Most of these 70-μm-excess galaxies are identified as $\sim L^*$ S0s with smooth profiles.

We find that almost every cluster galaxy in the process of star formation quenching is already either an S0 or Sa, while we find no passive galaxies of class Sb or later. Hence the formation of passive early-type galaxies in cluster cores must involve the *prior* morphological transformation of late-type spirals into Sa/S0s, perhaps via pre-processing or the impact of cluster tidal fields, before a *subsequent* quenching of star formation once the lenticular encounters the dense environment of the cluster core. In the cases of many cluster S0s, this phase of star formation quenching is characterized by an excess of 70-μm emission, indicating that the cold dust content is declining at a *slower* rate than star formation. We suggest that the excess 70-μm emission during quenching is due to either (i) a reduction of the star formation efficiency as proposed within the morphological quenching scenario or (ii) a 2–3 times increase in the dust-to-gas ratio or metallicity of the remaining interstellar medium, as predicted by chemical evolutionary models of galaxies undergoing ram-pressure stripping or starvation.

Key words: galaxies: clusters: general – galaxies: clusters: individual: A3558 – galaxies: clusters: individual: A3562 – galaxies: evolution – galaxies: star formation – infrared: galaxies.

1 INTRODUCTION

The evolution of a galaxy is a product of both nature and nurture – both of its mass, and of the environment in which the galaxy finds itself. Understanding the relative importance of nature and nurture remains a key issue in extragalactic astrophysics. These factors control the star formation rate (SFR) and the dynamical structure or morphology of the galaxy. In isolated galaxies, these observational quantities are largely determined by feedback processes acting within the interstellar medium (ISM) of the galaxy adjoined to its assembly history via mergers. In the harsh cluster environment,

★E-mail: cphaines@as.arizona.edu

star formation (SF) activity in infalling spiral galaxies can be both enhanced through collisions (Moss 2006; Bretherton et al. 2010) or quenched by various physical mechanisms such as ram-pressure stripping, harassment or starvation which transform them into the passive lenticulars which dominate the dense cluster cores (for reviews, see e.g. Treu et al. 2003; Boselli & Gavazzi 2006; Haines et al. 2007). These environmental mechanisms produce the well-known SF–density (e.g. Dressler, Thomson & Schechtman 1985; Poggianti et al. 1999; Balogh, Navarro & Morris 2000; Haines et al. 2009) and morphology–density (Dressler 1980; Dressler et al. 1997; Smith et al. 2005) relations. However, the dominant evolutionary pathway(s) which generates these relationships remains uncertain.

Moreover, it remains unclear whether these two relations are driven by the same process, by independent processes acting on diverse time-scales, or if one effectively drives the other. While some of the diminution in SF seen in cluster galaxies with respect to the field population could be attributed to the different morphological compositions of the two environments, even at fixed morphology, the SFR of cluster galaxies is found to be lower than in the field (Balogh et al. 2000), indicating separate processes at least partially shape these relations. Alternatively, Martig et al. (2009) suggest that it is the morphological transformation of spirals into S0s and the growth of the stellar bulge which drives the quenching of SF in lenticulars by making the gas disc more stable against collapse and fragmentation into star-forming clumps, without requiring gas consumption or removal. This interpretation is supported by the trend for the molecular gas consumption time-scale to increase systematically with galaxy concentration index (R_{90}/R_{50}), recently observed by Saintonge et al. (2011).

This quenching itself is not related to the environment of the galaxy, and so cannot alone explain the SFR–density relation, instead requiring some additional environmental process(es) capable of producing the prior morphological transformation of the galaxies, such as the impact of cluster tidal fields (Byrd & Valtonen 1990) or pre-processing within infalling groups (Balogh et al. 2004).

Infalling spirals in local clusters show evidence for the ongoing removal of gas via ram-pressure stripping (Crowl & Kenney 2008), leading to a rapid termination of SF from the outside-in, and subsequent fading of the disc component. However, S0s are found to differ from normal spirals due to higher bulge luminosities rather than fainter discs (Christlein & Zabludoff 2004), requiring bulge growth during S0 formation, disfavouring ram-pressure stripping or starvation models. Instead the increased scatters seen in cluster S0 and spiral Tully–Fisher relations support mechanisms that kinematically disturb infalling spirals, such as merging or harassment (Moran et al. 2007). Such tidal interactions are capable of channelling material to a central bulge sufficient to produce the higher central mass densities ($V_{\rm rot}^2/Gr_{\rm e}$) seen in cluster spirals (Moran et al. 2007) and ultimately the central surface brightnesses and stellar phase densities found in S0s.

A number of studies have attempted to distinguish among the various environmental processes by identifying and classifying various promising classes of transition galaxies, such as post-starburst and/or E+A galaxies (Dressler & Gunn 1983; Poggianti et al. 1999; Mercurio et al. 2004; Mahajan, Haines & Raychaudhury 2010, 2011), interaction-induced starbursts (Moss 2006; Fadda et al. 2008), and passive/red spirals (Van den Bergh 1976; Bamford et al. 2009), indicating that more than one mechanism is required.

A key diagnostic to understand the relevance of these proposed transition galaxies is mid-infrared (MIR) data to account for the dust-obscured SF. Many 'post-starburst' galaxies identified by their deep Hδ absorption lines and lack of O II emission were revealed by MIR data to be dusty starbursts (Duc et al. 2002; Dressler et al. 2009), whose age-dependant dust obscuration preferentially hides the young stars responsible for the OII emission above those older stars responsible for the Balmer absorption (Poggianti & Wu 2000). These spectroscopic and MIR surveys revealed a ubiquitous population of starburst and post-starburst $\sim L^*$ spirals in $z \sim 0.5$ clusters (Couch & Sharples 1987; Geach et al. 2006; Dressler et al. 2009), which are absent in present epoch clusters (Poggianti et al. 1999). They have been identified as the likely progenitors of present-day cluster S0s, whose populations have risen dramatically over the last 5 Gyr, empirically replacing the spirals (Dressler et al. 1997; Treu et al. 2003; Smith et al. 2005). Additionally, interaction-induced starbursts are often highly obscured (Mihos & Hernquist 1994), while many red-sequence galaxies (including spirals) have been revealed to be actively star forming, their red colours being attributed to dust obscuration rather than being passively evolving (Wolf, Gray & Meisenheimer 2005; Wolf et al. 2009; Haines et al. 2010).

Most previous studies of environmental effects on galaxies have concentrated on their impact on morphology and SF. However, given that the environmental processes behind the SF–density relation are likely to act *directly* on the ISM rather than the star-forming regions themselves, to fully understand the origin of the SF–density relation requires also measures of these impacts of environment on the ISM which subsequently drive it. To date, a detailed knowledge of the impact of environment on the ISM and dust content and how this drives the SFR–density relation is still largely lacking.

The most accessible probe of the ISM in distant galaxies is via far-IR (FIR) observations of the thermal emission from their dust contents. Using early *IRAS* (Neugebauer et al. 1984) and submm observations, Désert, Boulanger & Puget (1990) modelled the origin of the FIR emission in terms of two main components [ignoring polycyclic aromatic hydrocarbons (PAHs) here]: a warm component of small dust grains in H II regions heated by SF and a cool cirrus component of large dust grains heated by the interstellar radiation field (ISRF). Lonsdale Persson & Helou (1987) estimated that this cool, cirrus component contributes as much as 50–70 per cent of the FIR flux, while Sauvage & Thuan (1992) revealed a strong morphological trend, with a decreasing cirrus contribution from ~85 per cent for Sa galaxies to just 3 per cent for Sdm galaxies. The unprecedented wavelength coverage and sensitivity of *Herschel* (Pilbratt et al. 2010) allows us to extend these analyses to large samples of galaxies. Kramer et al. (2010) demonstrate the requirement of a two-component dust model to fit the 24–500 μm spectral energy distribution (SED) of M33, comprising a hot component (~60 K) tracing SF and a dominant cold component of large dust grains heated by the general ISRF. This second component can in effect measure the fuel available for SF, and a comparison of the two components allows us to measure the SF efficiency or gas consumption time-scale.

Using *IRAS*, Doyon & Joseph (1989) found that H I-deficient galaxies in the Virgo cluster had lower 60- and 100-μm fluxes, and cooler FIR colours than those with normal H I content. They interpreted this as evidence for the same two-component model for the FIR emission. In the cluster environment, the warm SF component is diminished in proportion to the H I deficiency suggesting that SF is regulated by the amount of available gas, while the cool component from diffuse dust is reduced by a smaller factor as dust is stripped from the galaxy. *Infrared Space Observatory* (*ISO*) extended the FIR coverage beyond that of *IRAS* to 240 μm, revealing the presence of a significant cold dust component (15–20 K) in a complete sample of 38 late-type Virgo cluster galaxies (Popescu et al. 2002).

While the MIR coverage of *Spitzer*/MIPS is dominated by the reprocessed dust emission from current SF, particularly at 24 µm, for the 70-µm band, typically ∼40 per cent of the integrated light from galaxies can be attributed to dust heated by the diffuse interstellar radiation from evolved stars (Bendo et al. 2010; Calzetti et al. 2010; Li et al. 2010). Hence the MIR colours (f_{70}/f_{24}) can be considered as a sensitive probe of the interrelation between the ISM and SF in galaxies.

In this paper we examine the MIR colours of galaxies in the Shapley supercluster core (SSC) at $z = 0.048$, the most massive and dynamically active structure in the local ($z < 0.1$) Universe (Raychaudhury 1989). In this paper, the SSC refers to a chain of three merging clusters, A3558, SC 1327−312 and SC 1329−313, along with the two associated Abell clusters on either side, A3562 and A3556. In Section 2 we present the panoramic *Spitzer* and ancillary data obtained within the ACCESS[1] multiwavelength survey used in this work. In Section 3 we present the MIR colours (f_{70}/f_{24}) of galaxies in the SSC, identifying a subpopulation with much redder IR colours ($f_{70}/f_{24} \gtrsim 25$) than can be reproduced by any of the standard IR SED models, before examining in detail the nature of these objects. In Section 4 we discuss possible origins of these 70-µm-excess galaxies, which appear to be dust-rich S0s yet with extremely low SFRs, before examining their consequences for the possible evolutionary pathways in the formation of cluster S0s. When necessary, we assume $\Omega_M = 0.3$, $\Omega_\Lambda = 0.7$ and $H_0 = 70\,\mathrm{km\,s^{-1}\,Mpc^{-1}}$, such that at the distance of the Shapley supercluster 1 arcsec is equivalent to 0.96 kpc.

2 DATA

The SSC was observed by *Spitzer*/MIPS in medium scan mode over 2008 August 27–30 within the Cycle 5 GO programme 50510 (PI: C.P. Haines). The observations consist of five contiguous mosaics providing homogeneous coverage of a ∼3 deg^2 region at both 24 and 70 µm, with effective exposure times per pixel of 84 and 42 s in the two bands, respectively. The data were reduced and analysed as described in Haines et al. (2011a, hereafter Paper II), producing catalogues which are 90 per cent complete to 0.35 mJy at 24 µm [corresponding to $L_{\mathrm{IR}} = 7.5 \times 10^8\,\mathrm{L_\odot}$ or SFR $= 0.05\,\mathrm{M_\odot\,yr^{-1}}$ based on the templates of Rieke et al. (2009)] and 25 mJy at 70 µm (corresponding to $L_{\mathrm{IR}} = 5.7 \times 10^9\,\mathrm{L_\odot}$). The MIR sources are then cross-correlated with optical *B*- and *R*-band imaging from the Shapley Optical Survey (SOS; Haines et al. 2006; Mercurio et al. 2006) and near-IR *K*-band imaging (Merluzzi et al. 2010, hereafter Paper I), which cover the same region (see fig. 1 in Paper II; Fig. 3).

We have spectroscopy of 814 supercluster members, of which 396 and 165 are detected at 24 and 70 µm, respectively. Of the 814 galaxies with redshifts placing them in the SSC, 415 come from the AAOmega-based spectroscopic survey of Smith, Lucey & Hudson (2007), for which high signal-no-noise ratio (S/N) spectra (median 60 Å^{-1}) were obtained via 8-h long exposure times. The 580V grating on the blue arm of the spectrograph provided wavelength coverage over 3700–5800 Å sample at 1 Å pixel^{-1}, while the 1000R grating on the red arm covered 5800–7300 Å at 0.6 Å pixel^{-1} (1.9 Å full width at half-maximum, FWHM).

In Haines et al. (2011b, hereafter Paper III), we found a clear bimodality in the IR colour f_{24}/f_K of SSC galaxies (shown here in Fig. 1). This ratio is a proxy for the SFR per unit stellar mass that can be used to separate passive ($f_{24}/f_K \simeq 0.1$) and star-forming ($f_{24}/f_K \simeq 2$) galaxies as discussed in detail in Paper III. This diagnostic also allows us to identify galaxies in between the two sequences, located in the IR analogue of the 'green valley' ($f_{24}/f_K \simeq 0.15$–1.0) population of UV–optical surveys. These galaxies are interpreted as being in the process of having their SF quenched.

[1] A Complete Census of Star-formation and Nuclear Activity in the Shapely Supercluster, http://www.na.astro.it/ACCESS

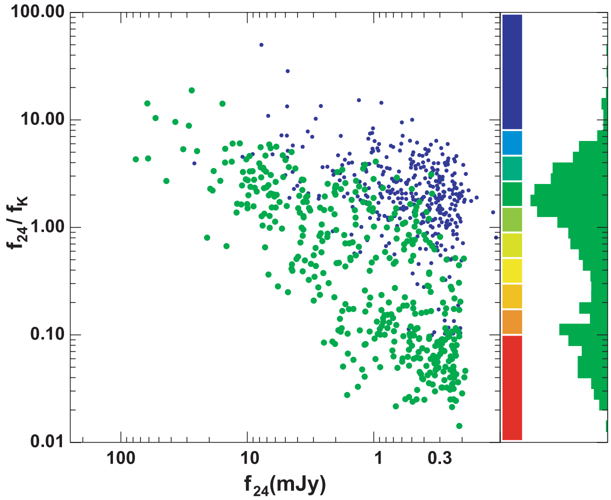

Figure 1. The IR colour f_{24}/f_K versus f_{24} for Shapley supercluster galaxies identified spectroscopically (large green symbols) and photometrically according to their UV–optical colours (blue symbols). The histogram shows the distribution of f_{24}/f_K colours of the 24-µm-detected supercluster galaxies, demonstrating the clear bimodality in the IR colours of supercluster galaxies. The vertical band indicates the colour scheme used in Fig. 2 to distinguish galaxies according to their f_{24}/f_K flux ratio.

3 RESULTS

3.1 Mid-infrared colours

In Fig. 2 we plot the MIR colour f_{70}/f_{24} versus 70-µm flux of spectroscopically confirmed (solid symbols) and photometrically selected (open symbols) Shapley supercluster galaxies (see Paper II). Each symbol is coloured according to its f_{24}/f_K flux ratio, as indicated by the coloured band of Fig. 1. Galaxies which belong to the star-forming sequence of Fig. 1 (green/blue symbols) generally have $f_{70}/f_{24} \sim 8$–20, consistent with colours predicted by the luminosity-dependent SEDs of Rieke et al. (2009) (magenta curve) and also the Dale & Helou (2002) models with $\alpha \gtrsim 1.5$. The latter are indicated by the red scale for $\alpha = 0.1$–4, and show a turn over at $\alpha \sim 2.5$. These SEDs are based on *IRAS* and *ISO* observations of 69 normal star-forming galaxies (Dale et al. 2001) and further calibrated with submillimetre observations. This α value parametrizes the distribution of dust mass as a function of heating intensity, as described in Dale & Helou (2002), in which values of $\alpha \gtrsim 2$ (as seen for most of our star-forming galaxies) indicate dust heating by low-intensity radiation typical of quiescent SF extended over a spiral disc. The bluest MIR colours ($f_{70}/f_{24} \lesssim 8$) imply smaller values ($\alpha \lesssim 1.5$), which correspond to more heating from stronger ISRFs, such as those produced by active galactic nucleus (AGN) or nuclear starbursts. Very few galaxies from our sample show such blue colours.

We note here a general trend for galaxies to have cooler f_{70}/f_{24} colours with decreasing f_{24}/f_K flux ratios. This would be expected for galaxies of a given mass/size as when their SFRs decline the

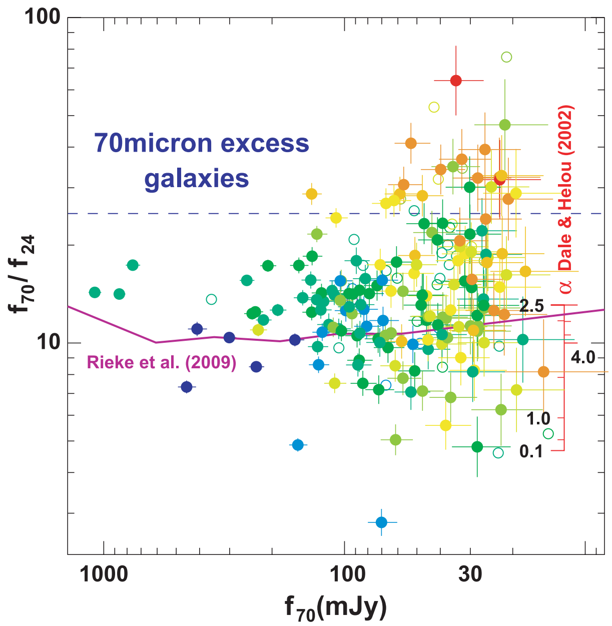

Figure 2. MIR colour f_{70}/f_{24} versus 70-μm flux of spectroscopically confirmed (solid symbols) and photometrically selected (open symbols) Shapley supercluster galaxies. Each symbol is coloured according to its f_{24}/f_K flux ratio, as indicated by the coloured band of Fig. 1. The magenta curve shows the predicted f_{70}/f_{24} colour evolution of the luminosity-dependent IR SEDs of Rieke et al. (2009). The red scale shows the expected MIR colours of the Dale & Helou (2002) models for $\alpha = 0.1$–4.

intensity of the SF and ionizing UV radiation reduces, leading to a decline in the overall dust temperatures.

We draw the reader's attention to the significant population of cluster galaxies with much redder IR colours ($f_{70}/f_{24} \gtrsim 25$; above blue dashed line) that appear inconsistent with any of the Rieke et al. (2009) or Dale & Helou (2002) SEDs at $\gtrsim 3\sigma$ significance levels. In total, we identify 23 '70-μm-excess' galaxies in the SSC having $f_{70}/f_{24} > 25$ or 14 ± 3 per cent of the 70-μm-detected SSC galaxies. We have visually checked the *Spitzer* maps and confirm that for each of these 23 sources corresponds to a clear, unambiguous detection in both 24- and 70-μm images, with no possible issues with deblending or merging with other sources. The spatial offsets between the 70 and 24 μm/K-band source positions of the 70-μm-excess sources (∼1–3 arcsec) are entirely consistent with those found for the remainder of the 70-μm sources of similar flux levels, and expectations of positional uncertainties based on their S/N levels. Our 70-μm images are far too shallow to be affected by confusion noise ($\sigma_c \sim 0.3$ mJy; Frayer et al. 2006). As such we would expect that their anomalously red colours are not simply the result of photometric uncertainties, whereby the 70-μm-excess is produced by low S/N sources whose 70-μm fluxes and f_{70}/f_{24} flux ratios have been scattered up by statistical fluctuations.

To ensure that this is indeed the case, we created random samples based upon the observed 24-μm fluxes and f_{70}/f_{24} distribution of the supercluster galaxies, after censoring the 70-μm-excess population. We then give each galaxy an artificial f_{70}/f_{24} value assuming a lognormal distribution ($\mu = 12.63$, $\sigma = 0.144$ dex) derived from the observed values, and then perturb both the 24- and 70-μm fluxes according to the observed photometric uncertainties (figs 5 and 8 from Paper II). After taking into account the completeness of our observed catalogues as a function of actual 70-μm flux, we estimate that we would expect ∼3 *detected* galaxies to have $f_{70}/f_{24} > 25$ due to being in the tail of the intrinsic f_{70}/f_{24} distribution, while ∼3 more would be scattered up into our sample by photometric uncertainties. We thus confirm that these 70-μm-excess galaxies are a real subpopulation.

Of the 22/23 galaxies with K-band photometry, 16 can be characterized as being $\sim L^*$ galaxies, having K-band magnitudes in the range 11.3–12.8, placing them within ∼1 mag of M_K^* (Paper I), the remainder forming a faint-end tail. It is notable that most of these galaxies lie in the transition region between the passive and star-forming sequences of Fig. 1 (as indicated by their yellow/orange symbols in Fig. 2), which could be interpreted as them being in the process of shutting down their SF via their interaction with the dense cluster environment. Such galaxies appear similar to the population of cluster galaxies with unexpectedly high $f_{100}/f_{24} > 30$ flux ratios identified in recent *Herschel* observations of clusters at $z \sim 0.2$ (Pereira et al. 2010; Rawle et al. 2010b; Smith et al. 2010). Overall, in terms of a mass-limited cluster galaxy population the 70-μm-excess galaxies make up 8 ± 2 per cent of all $K < 13$ ($M_K < M^* + 1.3$) SSC galaxies. It is difficult to assess if and how this population extends to lower masses, as they are likely to drop below our 70-μm survey limit beyond $K \gtrsim 13.5$, based on their expected IR colours.

We present the photometric properties of these 23 supercluster galaxies with $f_{70}/f_{24} > 25$ in Table 1, including their position, morphology and bulge-to-total ratio (as determined in Section 3.6), K-band magnitude, f_{70}/f_{24} and f_{24}/f_K flux ratios and NUV − R colour.

3.2 The environments of 70-μm-excess galaxies within the SSC

We plot in Fig. 3 the spatial distribution of the 70-μm-detected galaxies across the Shapley supercluster, colour-coded according to their f_{70}/f_{24} flux ratio from blue ($\lesssim 7$) through the typical ratios of normal star-forming galaxies in green (10–20) and the 70-μm-excess galaxies in yellow/orange/red ($f_{70}/f_{24} \gtrsim 25$). The 70-μm-excess galaxies are much more clustered than the overall 70-μm supercluster galaxy population, concentrated predominately towards the core of the richest cluster Abell 3558, along with others near the cores of both Abell 3562 and SC 1329−313.

To quantify this apparent clustering towards the cluster cores, we plot in Fig. 4 the cumulative distribution of distances of each 70-μm-excess galaxy ($f_{70}/f_{24} > 25$) from their nearest cluster in units of r_{500} (blue dashed curve), where the r_{500} values are estimated from mass density profiles derived from *Chandra* X-ray data (Haines et al. 2009). By comparing this to the corresponding distribution for all confirmed 70-μm-detected supercluster members (black solid curve), we see that the 70-μm-excess galaxies are on average at smaller clustercentric radii, with 60 per cent of them within 0.5 r_{500} as opposed to 25 per cent for the entire 70-μm-detected population. Using the two-sample Kolmogorov–Smirnov (KS) test, we estimate the significance of this result, finding $P_{KS} = 0.00077$ (3.36σ). Repeating this test, we find the 70-μm-excess galaxies more concentrated towards the cluster cores also than the general supercluster population (i.e. all spectroscopic supercluster members), albeit at less significance ($P_{KS} = 0.029$; 2.2σ).

3.3 Comparison to field galaxy samples

Are these 70-μm-excess galaxies purely a cluster phenomenon, or are they ubiquitous? To attempt to answer this, we have examined the IR colours of local field galaxies taken from the SIRTF Nearby Galaxy Survey (SINGS) (Kennicutt et al. 2003) and *Spitzer*

Table 1. Photometric properties of the supercluster members with $f_{70}/f_{24} > 25$. Where no near-UV (NUV) detection is made, we adopt a lower limit based on the NUV completeness limit of 22.0.

ID	RA (J2000)	Dec. (J2000)	Morph	(B/T)	Velocity	K	f_{70} (mJy)	f_{70}/f_{24}	f_{24}/f_K	NUV − R
5587	13:33:19.807	−31:39:40.440	S0	–	14 000	12.819	22.74	32.31	0.144	>6.38
6222	13:33:11.698	−31:40:09.195	E-S0	0.757	14 371	12.200	47.48	28.35	0.193	5.729
13898	13:35:18.317	−31:25:34.070	E-S0	–	14 863	–	64.33	41.81	0.000	6.220
22004	13:32:14.399	−31:22:57.368	S0	0.515	14 797	12.048	22.64	31.78	0.072	5.513
30092	13:33:09.527	−31:36:12.070	S0	0.631	14 440	12.772	27.94	32.15	0.170	5.756
36655	13:31:33.506	−31:48:46.282	E	0.796	13 250	12.207	34.44	64.05	0.062	6.232
61446	13:27:13.632	−31:23:54.909	E-S0	–	14 246	12.418	39.83	34.14	0.165	5.524
63446	13:27:47.799	−31:24:50.303	S0	0.982	14 119	12.179	32.55	36.72	0.100	5.895
64370	13:28:12.948	−31:26:24.527	Sa	0.156	14 853	12.639	20.86	27.69	0.130	4.704
64703	13:26:31.124	−31:26:49.215	S0	–	13 896	14.176	19.38	28.86	0.479	4.346
65317	13:27:48.517	−31:28:45.618	S0	0.536	15 709	12.141	58.85	28.72	0.224	5.847
66331	13:26:47.152	−31:29:43.419	Sg	0.293	15 250	14.196	24.55	30.19	0.590	>4.96
67258	13:28:28.612	−31:32:04.525	S0	0.294	14 199	12.718	26.08	39.32	0.123	5.496
67346	13:27:34.943	−31:32:59.260	E-S0	0.662	12 815	11.748	56.74	30.67	0.141	5.281
67440	13:28:14.518	−31:32:47.027	Sa	–	14 518	12.356	62.27	27.41	0.303	>7.37
67459	13:28:02.561	−31:32:13.551	S0	0.699	13 846	12.484	67.25	26.86	0.376	5.077
71694	13:28:08.902	−31:40:52.153	S0	0.678	12 233	11.874	52.95	41.10	0.110	6.112
108346	13:29:15.186	−31:07:44.365	E	0.690	14 554	11.955	108.39	25.23	4.296	5.114
109544	13:29:34.225	−31:08:40.936	S0	0.619	14 278	13.553	22.24	32.69	0.273	5.011
129757	13:26:38.815	−31:10:16.229	I	0.035	14 150	15.225	30.21	30.12	1.878	1.507
131628	13:27:35.052	−31:15:41.428	S0-S	0.330	15 095	11.340	136.96	28.72	0.249	5.821
143443	13:29:37.430	−31:55:57.080	Sg	0.002	14 238	15.523	21.56	46.85	1.134	2.272
149556	13:28:46.500	−32:10:00.286	Sg	0.051	13 710	14.970	35.44	34.85	1.506	2.068

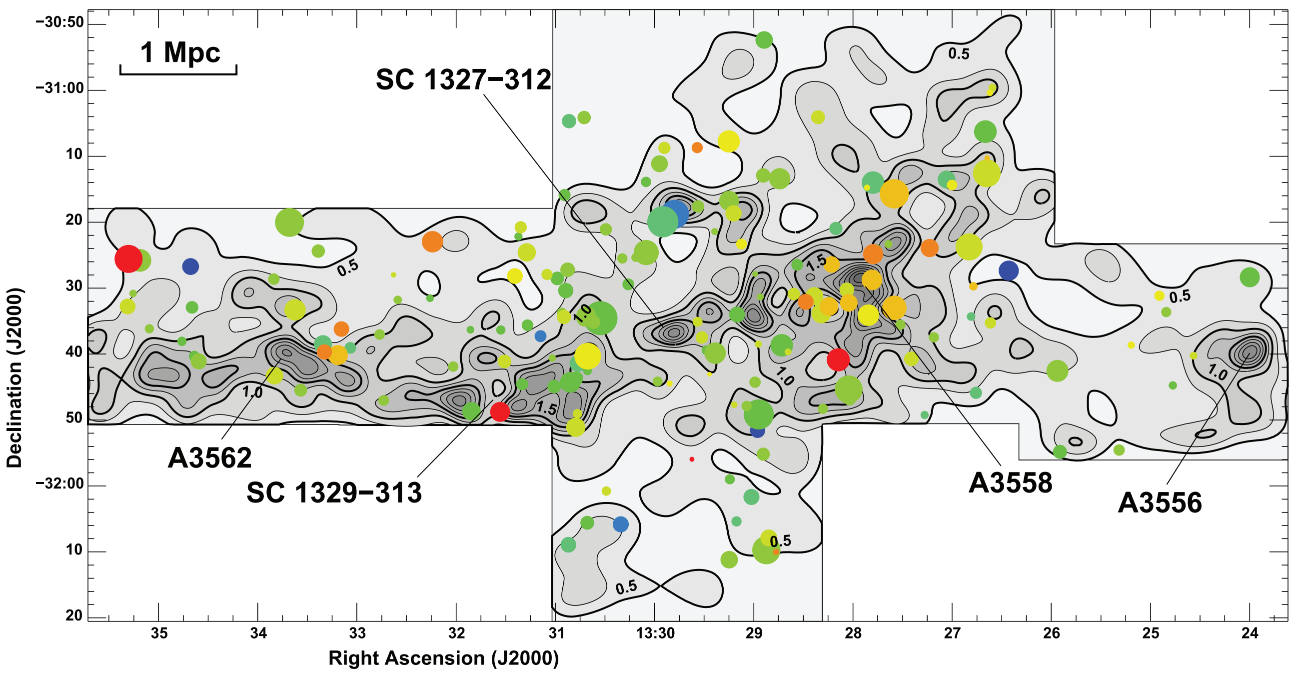

Figure 3. Spatial distribution of spectroscopically confirmed 70-μm sources across the Shapley supercluster. The symbols are coloured according to their f_{70}/f_{24} MIR colour from blue ($\lesssim$7) to orange/red ($\gtrsim$30), while the sizes scale with the K-band luminosity. The shaded region shows the coverage of WFI B-, R-band imaging from the SOS (Mercurio et al. 2006), from which we determine the morphologies. The grey-scale contours indicate the surface density of $R <$ 21 galaxies (fig. 1 of Haines et al. 2006).

Wide-area InfraRed Extragalactic (SWIRE; Lonsdale et al. 2003) surveys. After correcting the IR fluxes to the distance of the Shapley supercluster (to allow direct comparison with Fig. 2), we plot in Fig. 5 the f_{70}/f_{24} IR colour versus 70-μm fluxes of the SINGS galaxies as large symbols, coloured according to their morphological class. The bulk of the SINGS galaxies have the same IR colours as our observed star-forming sequence galaxies (green/blue symbols in Fig. 2) with $8 \lesssim f_{70}/f_{24} \lesssim 20$. We identify just one galaxy, the S0 galaxy NGC 5866, with the same anomalous red colour as our proposed 70-μm-excess population. Draine et al. (2007) identified NGC 5866 as a discrepant galaxy among their sample of 17 SINGS galaxies (mostly spirals) with Submillimetre Common-User

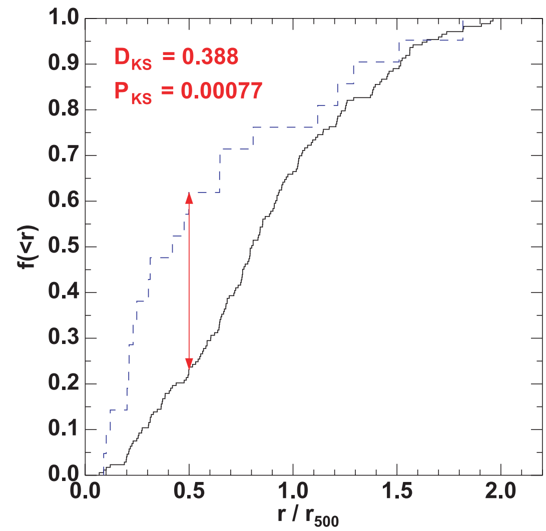

Figure 4. Cumulative distribution of the distances of 70-μm-excess (blue dashed curve) and all 70-μm-detected (black solid curve) supercluster members from their nearest cluster in units of r_{500}.

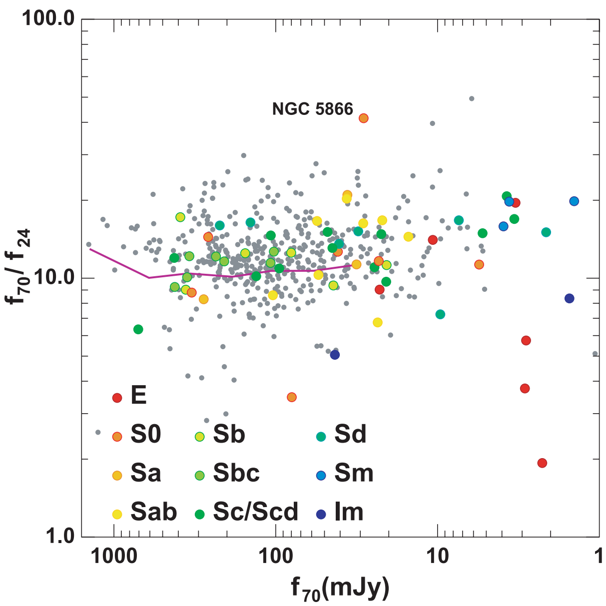

Figure 5. MIR colour f_{70}/f_{24} versus 70-μm flux of local field galaxies from the SINGS and SWIRE surveys. The large coloured symbols identify galaxies from the SINGS sample, where the colour of the symbol indicates the morphological class from red (E) to blue (Im). The smaller grey symbols indicate galaxies from the SWIRE survey with spectroscopic redshifts ($z < 0.12$) from SDSS. The f_{70} flux is based upon the galaxy being shifted to the distance of the Shapley supercluster.

Bolometer Array (SCUBA) submm photometry, due to its red f_{70}/f_{24} colour, and in fitting a dust model to the IR SED, required all of the dust to be exposed to a single diffuse ISRF, without any emission from dust heated by SF. Li et al. (2009) do however find evidence for low-level SF (SFR $\sim 0.05\,M_{\odot}\,yr^{-1}$) based on the detection of extended Paschen-α and Hα emission, while *Spitzer*/Infrared Spectrograph (IRS) spectroscopy reveals clear PAH features at 7.7, 11.3 and 12.7 μm due to SF (Shapiro et al. 2010).

We extend the field galaxy sample by matching the SWIRE 24- and 70-μm source catalogues for the Lockman and Elais N1/2 fields (Lonsdale et al. 2003) to the Sloan Digital Sky Survey Data Release 7 (SDSS DR7) optical spectroscopic and photometric catalogues (Abazajian et al. 2009), identifying 455 $z < 0.12$ galaxies with both 24- and 70-μm fluxes. Both the Lockman Hole and Elais N2 SWIRE fields fully lie within the SDSS DR7 footprint, covering 12.1 and 5.7 deg^2 respectively, while about one-fifth of the 8.5 deg^2 Elais N1 field also has SDSS spectroscopic coverage. We plot the FIR fluxes and colours of the SDSS–SWIRE matched sample as grey points in Fig. 5 after normalizing the MIR fluxes to those which would be obtained if the source were at the distance of the Shapley supercluster. The obtained f_{70}/f_{24} colours show a narrow range about the median value of 12.08, with 1σ and 2σ ranges of 9.25–16.5 and 5.3–24.8 respectively, fully consistent with the SINGS sample. We see a small population of hot IR-bright galaxies with $f_{70} > 100$ mJy and $f_{70}/f_{24} < 7$, for which the bulk of the IR emission is likely due to AGN. We confirm also the rarity of 70-μm-excess FIR-bright galaxies in the field, with just five of 420–440 sources (1.2 ± 0.5 per cent) in the SDSS–SWIRE matched sample that would have been detected above the completeness limit of our Shapley 70-μm imaging having $f_{70}/f_{24} > 25$. This evident rarity of 70-μm-excess sources in field surveys supports the hypothesis that these represent a cluster population.

3.4 Spectra

In Fig. 6 we present the spectra of all seven 70-μm-excess galaxies from the AAOmega survey of Smith et al. (2007) having $f_{70} > 30$ mJy. In the left-hand panel, we present the spectra from the blue arm, covering the region from rest-frame O II to O III, including the 4000-Å break and the age-sensitive Balmer indices Hδ, Hγ and Hβ (marked by the shaded vertical bands). For comparison, we show solar-metallicity simple stellar populations of ages 6 and 14 Gyr from the MILES evolutionary synthetic models (Vazdekis et al. 2010). Visually, these two models bracket and match well the overall continuum over this wavelength range as well as the primary age-sensitive features such as the 4000-Å break and the Balmer indices, suggesting that these galaxies are dominated by old stellar populations with ages in the range 6–14 Gyr. This can be shown also quantitatively, as four out of these seven galaxies with EW(Hα) < 0.5 Å had mean stellar ages determined by Smith et al. (2007), resulting in values of 6.3 ± 0.5 Gyr (# 6222), 9.8 ± 0.6 Gyr (# 13898), 11.0 ± 0.5 Gyr (# 63446) and 7.7 ± 0.7 Gyr (# 65317). There is also little, if any, evidence from the Rose Ca II indices (Leonardi & Rose 1996) of 'frosting' by small subpopulations of young stars (<1 Gyr), except perhaps for galaxy #61446, while equally there is no evidence of post-starburst signatures in the form of deep Balmer absorption lines.

In the right-hand panel, we present the spectra from the red arm covering the region around Hα for the same galaxies, again showing the 6- and 14-Gyr old SSPs for comparison. Even low levels of ongoing SF should be detectable in the form of Hα emission, but again we see little evidence for this in any of the galaxies except #61446, although there is apparent filling in of the Hα absorption expected of single old stellar populations. These galaxies have EW(Hα) in the range 0.3–3 Å and uncertainties of just 0.03–0.06 Å (Smith et al. 2007).

One caveat to this is that the AAOmega 2-arcsec diameter fibres cover just the central kpc of the galaxies, which can lead to severe aperture biases in the cases of galaxies with strong radial age or SF gradients (Kewley, Jansen & Geller 2005). In the case of early-type spirals or S0s, this could imply sampling only the central bulge, missing extended SF occurring within the outer disc and

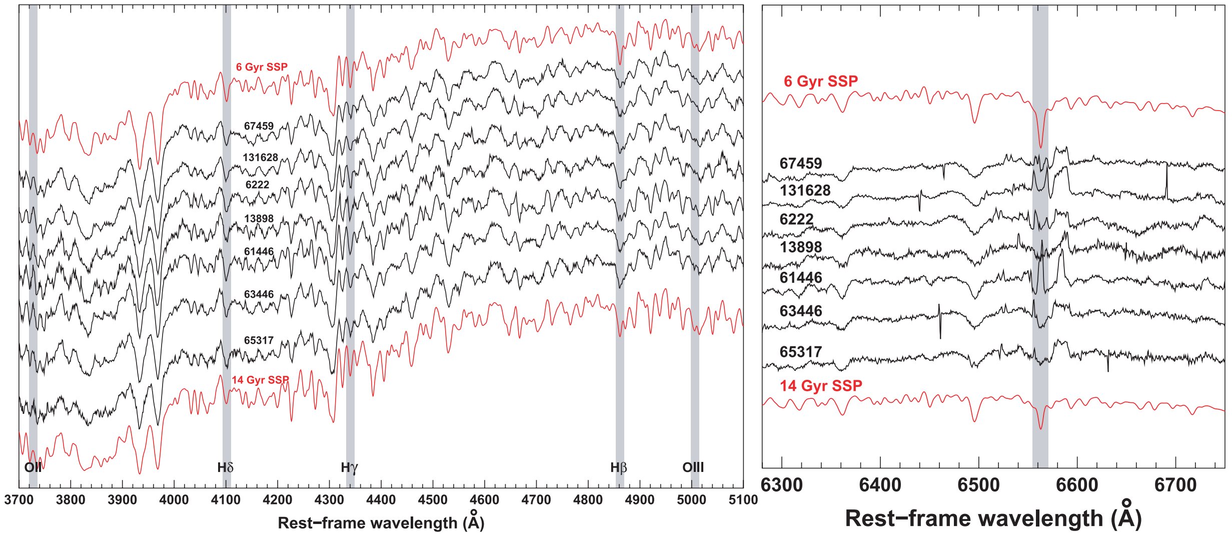

Figure 6. Optical spectra (shifted to the rest frame of the galaxy) of those 70-µm-excess supercluster galaxies within the AAOmega sample of Smith et al. (2007) covering the wavelength range 3700–5100 Å (left) around the Hα emission line (right). Also shown are two SSPs from the MILES stellar population models (Vazdekis et al. 2010) which bracket the properties of the observed spectra. The primary Balmer (Hα, Hβ, Hγ, Hδ) and forbidden-line (O II, O III) indices are indicated by shaded vertical bars.

spiral arms as demonstrated most clearly in Haines, Gargiulo & Merluzzi (2008). Rawle, Smith & Lucey (2010a) presented VIMOS integral field spectroscopy of three of the 70-µm-excess galaxies (#65317≡MGP 1626; #13898≡MGP 3976, #30092≡MGP 3971). They found no evidence for young stellar populations in the outer regions of these galaxies. Indeed MGP 1626 and MGP 3971 have the two strongest *positive* age gradients in their sample of 19 galaxies, i.e. the central regions covered by the AAOmega fibres map the youngest stellar populations in the galaxies. These three galaxies show no statistical differences in the radial gradients of any of the stellar population parameters (age, metallicity and abundances) or velocity dispersion from the remainder of the sample (T. Rawle, private communication). This global lack of SF in these galaxies is confirmed by their red NUV $- R \sim 5$–6 colours, placing them within the UV–optical red sequence (Haines et al. 2008).

In summary, both spectroscopic (both fibre-based and integral field) and UV continuum observations of the 70-µm-excess galaxies find them completely dominated by emission from evolved stars with little or no evidence of young stellar populations ($\lesssim$1 Gyr).

3.5 Panchromatic SEDs

We now attempt to gain insight into the origin of the MIR colours of these galaxies, by examining their panchromatic SEDs. In Fig. 7 we plot the SEDs of all the 70-µm-excess galaxies (with K-band photometry) from the far-ultraviolet (FUV) to the FIR, after normalizing at 2.2 µm (circular symbols). In order to efficiently model their SEDs, we have first split the population into two according to whether they appeared UV-dim (NUV $- R \gtrsim 5$; left-hand panel) or showed significant UV emission (NUV$-R \sim 2$; right-hand panel). In terms of numbers, the vast majority (19/22) of the 70-µm-excess galaxies fall in the UV-dim subpopulation, and so we will focus most attention on these.

We have modelled the averaged panchromatic SEDs of the two subpopulations by the starburst models of Groves et al.

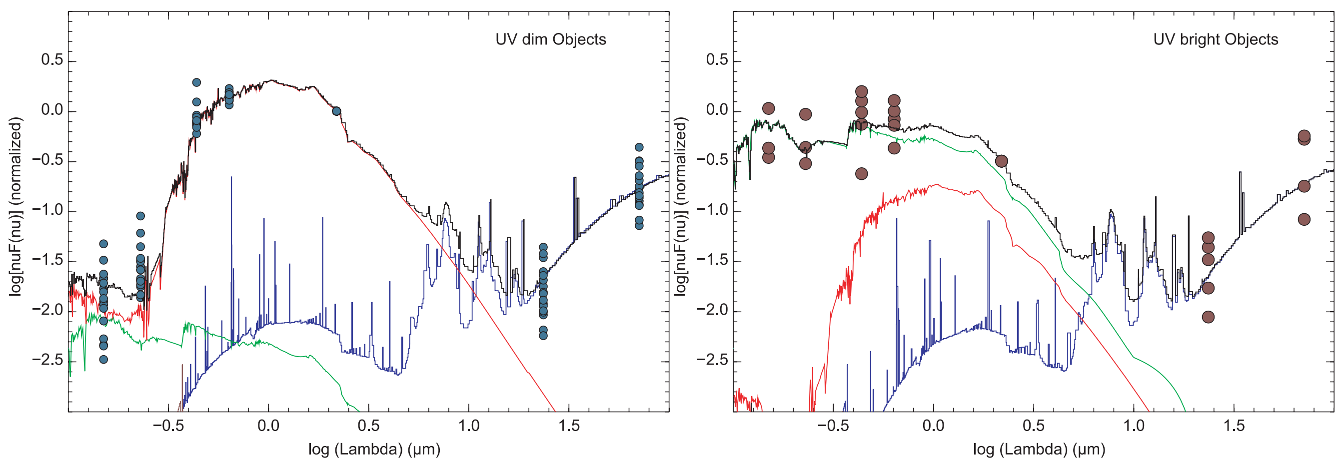

Figure 7. The best-fitting model (black curve) panchromatic FUV–FIR SED of the 70-µm-excess galaxies normalized at 2.2 µm (blue symbols) separated into those which are UV-faint (left-hand panel) and UV-bright (right-hand panel). The pan-spectral model SED is made up of three components: an 11-Gyr old stellar population (red curve); young 10–100 Myr old stellar population (green curve) and emission from the H II regions (blue curve).

(2008). These models combine the stellar spectral synthesis code STARBURST99 (Leitherer et al. 1999) and the photoionization code MAPPINGS III (Groves 2004), which follow both the nebular emission and radiative transfer locally within individual H II regions. The expansion of these regions is driven by the mechanical energy input of their cluster stars and supernovae (Dopita et al. 2005). The FUV–FIR SEDs of the 70-μm-excess galaxies were fitted by models with three components: (i) an ensemble of young H II regions surrounding young clusters with ages <10 Myr enclosed by photodissociation regions and foreground attenuation by a dust screen (blue curve); (ii) a young stellar population with ages 10–100 Myr modelling the young stars that have recently dispersed into the field from the active star-forming regions (green curve) and (iii) an old stellar population based on the 11-Gyr template of Bruzual & Charlot (2003) to model the evolved stars unconnected with the current SF episode (red curve).

In the UV–optical, we see little or no contribution from the current or recent SF to the spectra for the vast majority of these galaxies (left-hand panel), being essentially modelled by a simple stellar population of age 11 Gyr. This is particularly so for 0.3–3 μm, consistent with the observed AAOmega spectra being well described by 6–14 Gyr old SSPs (Fig. 6). Only in the FUV is any contribution from young (<100 Myr old) stars apparent, but even here it could be feasibly be excluded for many of the galaxies. This does not appear to be due to dust extinction, the underlying old stellar population is extinction free, while the modelled young 10–100 Myr old component has $A_V \sim 0.3$ mag. The models predict a negligible contribution at UV–optical wavelengths from H II regions, with little or no detectable nebular emission. This is confirmed by the lack of significant Hα emission in any of the galaxies in Fig. 6 or those covered by integral field (IFU) spectroscopy (Rawle et al. 2010a). Moreover, the optical and nebular emission suggested by the blue curves is an artefact of the models, which connect implicitly the dust heating process to H II regions, producing nebular emission as a consequence of the ionizing UV radiation (heavily extinct) required to heat the dust sufficiently to produce the observed FIR emission. Given the clear lack of observed UV or nebular emission, the origin of the UV/optical radiation required to heat the dust component remains unclear.

The emission from H II regions is instead only detectable in the MIR/FIR, demonstrating the importance of such data for fully understanding the processes which drive and quench SF in galaxies. The H II component indeed is required to fit the observed emission in the *Spitzer*/MIPS 24- and 70-μm passbands, the predicted 24-μm emission due to photospheric emission from the evolved stellar population (red curve) being an order of magnitude lower than that observed. The models also predict that emission from the H II regions should be detectable in the form of PAH emission at 6–20 μm. Unfortunately, we do not have any photometry at these wavelengths, although we note again that NGC 5866 from the SINGS sample does indeed show clear PAH features (Shapiro et al. 2010).

One caveat is that *Spitzer* IRS observations of early-type galaxies have revealed diffuse, excess emission over 10–30 μm, due to silicate emission from the dusty circumstellar envelopes of mass-losing asymptotic giant branch (AGB) stars (Bressan et al. 2006), which persists even for the very evolved stellar populations beyond 10 Gyr old (Piovan, Tantalo & Chiosi 2003). While this component is not included in our models, and could in principle explain the 24-μm fluxes, its emission should then decline rapidly beyond 30 μm, and hence could in no way contribute significantly to the thermal emission detected at 70 μm.

We do note however that 3/23 galaxies from our sample do have significant UV emission from recent SF (right-hand panel of Fig. 7), having NUV − $R \sim 2$. These three also have $f_{24}/f_K \sim 1.5$ ratios typical of normally star-forming galaxies, much lower K-band luminosities and later-type morphologies than the remainder of the sample. Given the rather diverse properties of these three galaxies with respect to all of the others, and the likelihood that many similar low-mass galaxies would be missed by our 70-μm survey, it is difficult to assess the importance or relation of these galaxies with respect to the rest of the population.

As well as providing a robust constraint for the level of SF within H II regions, the MIR emission constrains the intensity of the radiation heating the dust, via the compactness parameter, $\mathcal{C}$, which is of the form

$$\mathcal{C} \propto \frac{\langle L_*(t)\rangle}{\langle R(t)^2\rangle}, \quad (1)$$

where $L_*(t)$ and $R(t)$ describe the time evolution of the stellar luminosities and radii of the H II regions (Groves et al. 2008). Hence $\mathcal{C}$ provides a measure of the density of radiation within H II regions available for heating the dust. As is shown in fig. 5 of Groves et al. (2008), the primary effect of varying $\mathcal{C}$ is to change the temperature of the dust, and systematically shift the wavelength of the FIR dust emission. As the compactness parameter decreases from $\log \mathcal{C} = 6.5$ to 4.0, the peak wavelength of the FIR emission moves to progressively longer wavelengths from 50 to 130 μm, i.e. the dust temperature drops from ∼60 to ∼20 K. The constraint on the compactness parameter for our galaxies comes from their f_{70}/f_{24} colours, which can only be modelled by an extremely low compactness parameter $\log \mathcal{C} \sim 4.0$. Such a low $\mathcal{C}$ value produces dust temperatures and FIR SEDs similar to those produced by a radiation field of intensity 1–10 times the local ISRF, similar to that modelled for NGC 5866 (Draine et al. 2007). In contrast, SF within H II regions produces a more intense radiation field, heating the surrounding dust to higher temperatures, resulting in compactness parameters $\log \mathcal{C} \gtrsim 5.5$ (Dopita et al. 2011), inconsistent with our SED model fits. If we consider the predicted FIR colours of a galaxy with emission solely from the general ISRF, the maximal f_{70}/f_{24} ratio would occur for a radiation field ∼10 times the local 'solar neighbourhood' ISRF (Compiègne et al. 2011).

This view that the anomalous f_{70}/f_{24} colours require very low values of the compactness parameter $\mathcal{C}$ is consistent with the model predictions of Li et al. (2010) who show that the characteristics of the dust emission as observed by the f_{70}/f_{24} colour are strongly linked to the surface density of SF within a star-forming region (ΣSFR/M$_\odot$ yr^{-1} kpc^{-2}), independent of metallicity (their fig. 8). In this case, the 2–3 times increase in f_{70}/f_{24} required to produce our 70-μm-excess galaxies from the normal star-forming population implies a reduction in ΣSFR of ∼50–100 times. Similarly, Calzetti et al. (2010) show that the integrated f_{70}/f_{24} colours of normal star-forming galaxies (luminous infrared galaxies excluded) are tightly anticorrelated with the SF surface density (their fig. 17), while Popescu et al. (2011) show that the MIR colours mainly depend on the ratio between the diffuse component from the ISM (heated by both young and old stars) and the clumpy component from the H II regions (the F factor in their formulation). In this latter work, the largest f_{70}/f_{24} ratios are produced by a diffuse component heated only by evolved stars without a significant additional clumpy component.

We note at this point that there are clear limitations on our ability to model and constrain the FIR emission of these galaxies. First, given that we have just two data points (24 and 70 μm), we can only reasonably fit the FIR emission by a single-component model with one free parameter, $\mathcal{C}$. This means that we cannot consider more complex or realistic models which are able to fit separately the diffuse cool dust component related to the general ISM and the hotter, clumpy component linked to SF (e.g. Popescu et al. 2011). Moreover, the lack of coverage beyond 70 μm means that we are not mapping the peak of the FIR emission from large dust grains, and so cannot constrain either the temperature or mass of the cool, diffuse dust component. In particular, we cannot distinguish between models in which the excess 70-μm emission is due to an increase in the mass of the cold, diffuse dust component, or rather an increase in its temperature. While our MIR observations are sufficient to show that the IR (∼10–1000 μm) emission comes primarily from a cool diffuse component, further observations in at least one passband at ∼200–500 μm to map the Rayleigh–Jeans tail of the FIR emission are required to constrain the nature of this diffuse component, in a manner similar to that already achieved using *Herschel* PACS/SPIRE observations in five FIR bands over 70–500 μm (e.g. Kramer et al. 2010; Rawle et al. 2010b).

3.6 Morphologies

We morphologically classified each spectroscopic member of the SSC by eye, placing them on to the revised Hubble scheme (de Vaucouleurs 1959, 1963), using the high-quality *B*- and *R*-band WFI imaging from the SOS (FWHM ∼ 0.7 arcsec), extending the earlier morphological classification performed by Gargiulo et al. (2009) for the passively evolving subsample. The angular resolution and depth (Mercurio et al. 2006) of the data allow us to assign each galaxy into the following classes: E, E/S0, S0, S0/S and S. The spirals (S) are subsequently split into Sa, Sb, Sbc, Sc, Sg and Irregulars, where Sg are clearly spirals, but for which we could not make any more detailed classification. E galaxies have smooth radial profiles without discontinuities in surface brightness. S0 galaxies show a clear additional non-spheroidal (disc or lens) component, but no apparent spiral arms. E/S0 galaxies appear azimuthally symmetric, preventing us from visually distinguishing between Es and face-on S0s. The above classification scheme is identical to that used by Thomas & Katgert (2006) for a subset of 201 SSC members in the vicinity of A 3558 and A 3562 as part of the ESO Nearby Abell Cluster Survey (ENACS). This allows us to compare directly our morphologies with a completely independent set of classifications, albeit those of Thomas & Katgert (2006) are based on poorer quality *B*-, *R*-band imaging (1.2–2.0 arcsec) from the 1.54-m Danish Telescope at La Silla (Katgert et al. 1996). In general, we find excellent agreement between the two sets of classifications, although the improved image quality of our WFI images revealed a small fraction of galaxies classified as S0 or S0/S by Thomas & Katgert (2006) to be spirals.

Of the 23 SSC galaxies with $(f_{70}/f_{24}) > 25$, two were classed as Es, four as E/S0s, 11 as S0s, two as Sa and four later-type galaxies. The four late-types are the four lowest luminosity galaxies with $K > 14$. That the vast majority of these galaxies are of morphological class Sa or earlier would appear surprising given that all have 70-μm detections, even if we are sampling an overdense region where early-type galaxies should dominate. If we consider the morphologies of all 165 70-μm-detected SSC galaxies, 65 are E/S0s while 100 are spirals (Sa or later). Based on binomial statistics, there is a probability of just 3.4×10^{-4} of extracting 17 or more E/S0 galaxies out of 23 by chance from the global population. What is most notable is that for all these galaxies we see smooth surface profiles with no evidence of star-forming regions. This is particularly surprising given their 70-μm-based selection, as all previous morphological surveys of MIR/FIR or radio-selected cluster galaxies have been completely dominated by late types and mergers (Smail et al. 1999; Balogh et al. 2002; Coia et al. 2005).

To obtain a more quantitative measure of the morphological structures of these galaxies, we have performed a bulge–disc decomposition using 2DPHOT (La Barbera et al. 2008) to fit the *R*-band radial surface brightness profile of each galaxy. In Fig. 8 we show the one-dimensional radial *R*-band surface brightness profiles of 10/11 galaxies (black points) from our sample of 70-μm-excess galaxies with $f_{70} > 30$ mJy (we could not perform surface photometry on one galaxy due to it being near a bright star), in order of decreasing f_{24}/f_K and the best-fitting linear combination of a Sérsic profile (red curve; representing the bulge) and an exponential profile (blue curve; representing the disc), convolved with the local point spread function (PSF), as estimated from nearby non-saturated stars. In almost all cases we see the primary characteristics of S0s, with the central regions dominated by a high-surface brightness bulge component, which makes way to a dominant disc component characterized by a smooth exponential profile at larger radii.

Looking at the bulge–disc decompositions in order of decreasing f_{24}/f_K (from top left to bottom right) there visually appears some

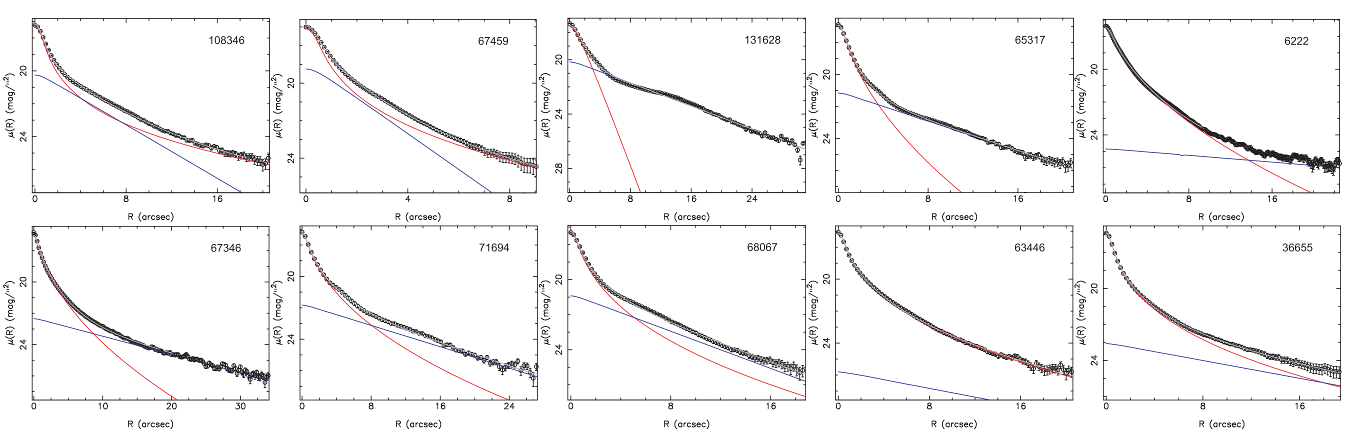

Figure 8. The bulge–disc decomposition of the 70-μm-excess galaxies in order of decreasing f_{24}/f_K, showing the *R*-band surface brightness profile, with resulting best-fitting bulge (red curve; Sérsic fit) and disc (blue curve; exponential) components.

trend for the bulge component to become increasingly dominant while the disc component declines. Although within these 10 galaxies we only see a marginal correlation between the bulge-to-total (B/T) ratio and f_{24}/f_K, being significant only at an 88 per cent level based on the Spearman rank correlation test, when considering the whole 70-µm-excess sample this significance increases to 97 per cent. This correlation suggests the SF is being quenched as the disc component declines and/or the bulge component is being built up in S0s. Alternatively, this trend could simply reflect that these are composite systems, comprising both bulge and disc components, with the 24-µm emission associated to the star-forming disc.

We also performed full two-dimensional surface photometry of the 70-µm-excess galaxies using the semi-automated GALFIT (v2; Peng et al. 2002) software. Thumbnails centred on each galaxy were extracted from the *R*-band images, and the surface photometry modelled as either exponential or Sérsic profiles, or a linear combination of the two, each convolved with the local PSF, the best fit obtained by minimizing the χ^2 residuals. In Fig. 9 we show four example fits obtained by GALFIT. In the top two rows, we show the original thumbnail image of the 70-µm-excess galaxy (left-hand panel), the residuals obtained after fitting with a single Sérsic model (central panel) and the residuals obtained after fitting with a linear combination of a bulge and disc component (right-hand panel). For these galaxies, we see that a single Sérsic model does not provide an accurate fit to the galaxy profile, simultaneously underestimating the galaxy flux along the major axis, while over-subtracting the flux along the minor axis. The remnants of a disc component are clearly visible. The combination of bulge and disc components perform much better, certainly along the minor axis, although even here we see clear residuals from either a boxy bulge or spiral arms. In the lower two panels, we simply show the original thumbnail image (left) and residual maps after subtracting the best-fitting bulge+disc model. In the first case we obtain an excellent fit, with almost no residuals, while for the second case there is evidence for a remnant bar.

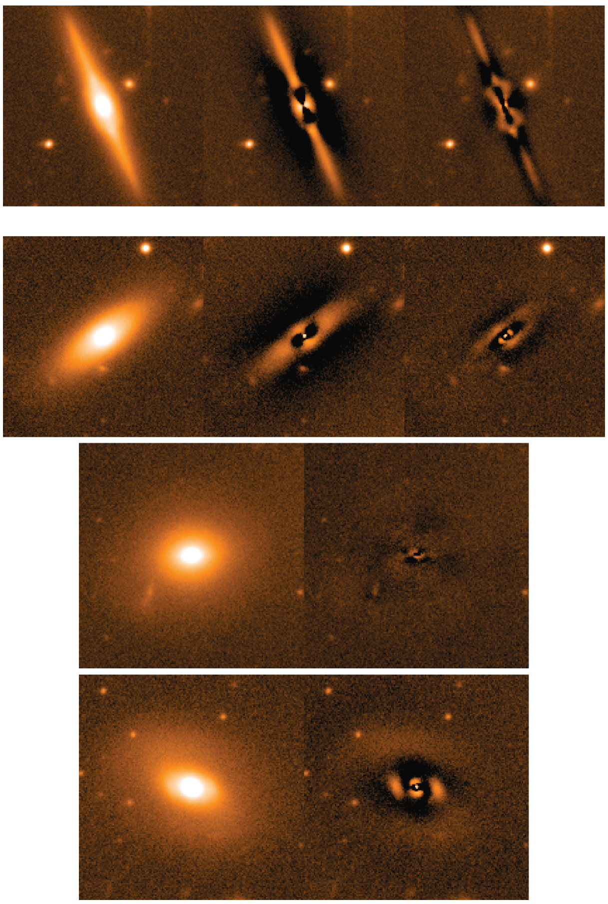

Figure 9. Sample two-dimensional fit results for 70-µm-excess galaxies. Each plot shows the *R*-band galaxy thumbnail (left) and residual map(s) (centre/right) after subtraction of the best-fitting GALFIT models), using the same grey-scale of intensity levels. The top two panels show the residual maps for both the best-fitting single Sérsic model (centre) and Sérsic+exponential disc models, while the bottom two panels show the residual maps for just the Sérsic+exponential disc model. The colour scaling is kept constant for each galaxy.

3.7 The 70-µm-excess phase along the quenching sequence

To place these 70-µm-excess galaxies along the evolutionary pathway from normal star-forming spiral to passive S0s, we plot in Fig. 10 f_{24}/f_K versus f_{70}/f_K flux ratios colour-coded according to their morphological classification. As discussed previously, we can consider the f_{24}/f_K ratio to be a good proxy for the specific SFR. The 70-µm emission could be better described as a measure of the cooler dust (20–60 K), either that belonging to the ISM or also that associated with the SF. For the spiral galaxy population (green/blue symbols), we can see the overall colour–colour trend can be well described a sequence in f_{24}/f_K in which the 70-µm emission is directly proportional to the 24-µm emission ($f_{70}/f_{24} = 10$; dashed line). This suggests that for these galaxies the 70-µm emission produced primarily from dust heated by SF.

However, at the lowest f_{24}/f_K ratios, we see the f_{70}/f_K ratios of the S0s (orange/yellow symbols) lie systematically above this sequence (although ellipticals in contrast do not), suggesting that the 70-µm emission is declining slower than the 24-µm emission. Following Doyon & Joseph (1989) who suggested that whereas

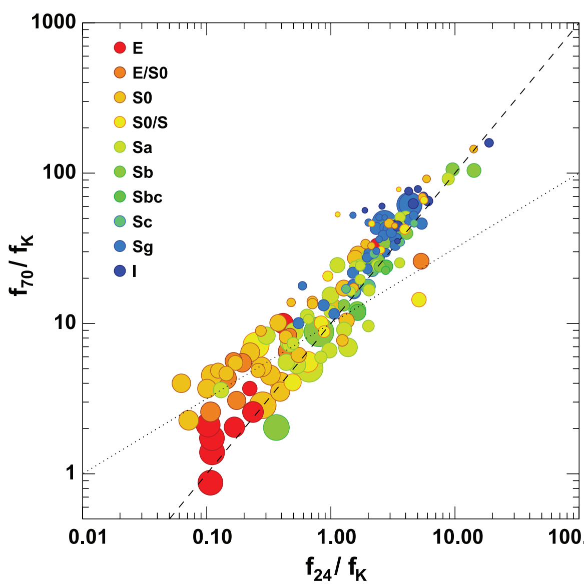

Figure 10. The IR f_{70}/f_K versus f_{24}/f_K colour–colour sequence for Shapley supercluster galaxies detected at 70 µm. The symbols are coloured according to their morphological classification, while the sizes scale with the *K*-band luminosity. The dashed line indicates the sequence with $f_{70}/f_{24} = 10$, while the dotted line indicates a sequence with $f_{70}/f_K \propto (f_{24}/f_K)^{1/2}$

the SF declines in a manner proportional to the H I deficiency, the cool dust content declines at slower rate. If we consider the f_{70}/f_K as a measure of the cool dust content, this would then decline as $(f_{24}/f_K)^{1/2}$, as shown in Fig. 10 by the dotted line. As da Cunha, Charlot & Elbaz (2008) and da Cunha et al. (2010) show, for actively star-forming galaxies stellar birth clouds are the main contributors to dust heating and hence the IR emission, while in more quiescent galaxies, the bulk ($\gtrsim$80 per cent) of dust emission arises from the heating of dust by older stars in the ISM. Indeed, for galaxies of a given stellar mass, they find (M_d/SSFR) $\propto$ SSFR$^{-1/2}$, and so for galaxies in which the 70-μm emission and dust heating is primarily due to evolved stars, we may expect the dust content and hence f_{70}/f_K to follow the dot–dashed curve. Interestingly, in a comparable *Spitzer*/MIPS analysis of 225 E/S0 galaxies, Temi, Brighenti & Mathews (2009) find a remarkably tight 'banana-shaped' relation among the IR colours formed by the f_{24}/f_K and f_{70}/f_K ratios. For E/S0s with f_{24}/f_K ratios lying within the transition region up to the normal star-forming sequence, shows the f_{70}/f_K ratio declining as $(f_{24}/f_K)^{2/3}$ before turning over and declining rapidly as the galaxy reaches the passive sequence in f_{24}/f_K.

The trends revealed by Fig. 10 support the 70-μm-excess population representing a fundamental aspect of the quenching of SF within early-type galaxies.

4 DISCUSSION

We examined the MIR colours of 165 70-μm-detected spectroscopic members of the SSC at $z = 0.048$, using panoramic *Spitzer*/MIPS 24- and 70-μm data. Among these galaxies, we identified a population of 23 '70-μm-excess' galaxies, comprising 14 ± 3 per cent of 70-μm-detected SSC galaxies, whose MIR colours ($f_{70}/f_{24} > 25$) are much redder than can be reproduced by any of the standard IR SED models, and which also appear extremely rare in field surveys. These galaxies are primarily massive $\sim L^*_K$ galaxies with E/S0 morphologies, and intermediate f_{24}/f_K ratios placing them in transition zone in which galaxies in the process of having their SF quenched are likely to be located. In the two-component model for the FIR emission, these colours could be understood as galaxies in which the SF is being quenched (or was recently), thus reducing the 24-μm emission and explaining the low f_{24}/f_K flux ratios, while the emission seen at 70 μm is largely due to dust heated predominately by relatively young stars (10^8–10^9 yr) and the ISRF.

These 70-μm-excess galaxies comprise 8 ± 2 per cent of all $K < 13$ ($M_K < M^* + 1.3$) SSC members, indicating that they represent an important evolutionary pathway for cluster galaxies. Given this, we now attempt to place these galaxies within the theoretical frameworks provided by the various environmental processes that are currently believed to be important in transforming galaxies within clusters, including ram-pressure stripping and morphological quenching.

4.1 Ram-pressure stripping

The concentration of these 70-μm-excess galaxies in the cluster cores would suggest ram-pressure stripping as the mechanism causing the observed quenching of SF. In such galaxies, the gas is stripped from the outside-in, leaving truncated H I discs (Vogt et al. 2004). Within this truncation radius SF continues normally, but outside evidence is found for recently quenched stellar populations (Crowl & Kenney 2008). Using spatially resolved *Herschel*/SPIRE maps Cortese et al. (2010a) show the cold dust to be collocated with the gas, appearing truncated for highly H I-deficient spirals in the Virgo cluster. Hence, while SF is quenched and gas removed via ram-pressure stripping, as the gas/dust surface densities within the truncation radius remain high, the SF *efficiency* should be unaffected, and the SFR and gas contents should decline in step.

While the H I gas contents of cluster galaxies may be partially or completely stripped by ram-pressure, the molecular gas, by virtue of its much higher density and being more tightly bound within the potential well of the galaxy, should be much more difficult to remove. Indeed, in a CO survey, 260 early-type galaxies from the volume-limited ATLAS^{3D} sample, Young et al. (2011) recently found no significant difference between the molecular gas contents of early-type galaxies in the Virgo cluster and those in isolated field regions within 24 Mpc. Moreover, the dynamical status of the 12 CO-detected Virgo cluster galaxies (all S0s) is consistent with being a virialized population, deeply embedded within the hot intracluster gas, and unlikely to be recently accreted cluster members. They have probably retained their molecular gas over several Gyr within the cluster, albeit their molecular gas fractions ($M_{H_2}/M_* \sim 0.001$–0.01) are now a factor $\gtrsim$10 times lower than those of normal star-forming galaxies (Saintonge et al. 2011).

As ram-pressure stripping and the milder starvation mechanism prevent further accretion of pristine gas, the remaining H I gas is enriched by metals recycled from stellar mass loss, particularly via the shedding of the stellar envelopes during the AGB phase, increasing the gas metallicity by a factor ∼2–3 (Skillman et al. 1996; Boselli et al. 2008), which may in turn reduce the SF efficiency (and hence 24-μm emission) by a similar factor (Dib et al. 2011). As the dust-to-gas ratio is known to scale approximately linearly with metallicity (Draine et al. 2007), we may expect the ratio between dust content and SFR to increase by a similar factor 2–3. This however requires us to make many assumptions about how the metals produce by evolved stars are frozen into dust grains, as well as the rate at which dust grains are destroyed in the ISM for S0s passing through the cores of clusters as opposed to isolated field spirals. This enrichment of the remaining ISM by stellar mass loss could though be responsible for the anomalously red f_{70}/f_{24} colours. Moreover, an increase in the dust-to-gas ratio may directly reduce the SF efficiency, if radiation pressure from the absorption and scattering of starlight by dust grains acts as an important mechanism in regulating SF (Andrews & Thompson 2011).

Leitner & Kravtsov (2011) show that at low redshifts gas recycling from stellar mass loss can provide most if not all of the gas required for SF in galaxies, particularly those with lower than average specific SFRs (as our galaxies are). The key for stellar mass loss to be efficient in fuelling SF is the presence of at least some gaseous disc, into which the enriched material can be released directly. For elliptical galaxies with hot gas haloes, the enriched gas released by AGB stars is likely rapidly disrupted and mixed with the hot halo gas. The simulations of Martig & Bournard (2010) suggest that continuous recycling of gas through stellar mass loss also contributes significantly to the growth and survival of the disc component in these cluster S0s. Davis et al. (2011) find that the molecular gas of the Virgo cluster CO-detected S0s is always kinematically aligned with the stellar kinematics, consistent with an internal origin such as stellar mass loss.

Another explanation could be that the cold dust is heated during the stripping process, boosting the 70-μm fluxes. This would be consistent with the 100-μm-excess galaxies found by Rawle et al. (2010b) in the Bullet cluster, as the dust temperatures estimated by their fitting, their combined *Herschel*/PACS+SPIRE photometry for these galaxies, were found to be higher than expected given their IR luminosity. The ram-pressure could also be removing the

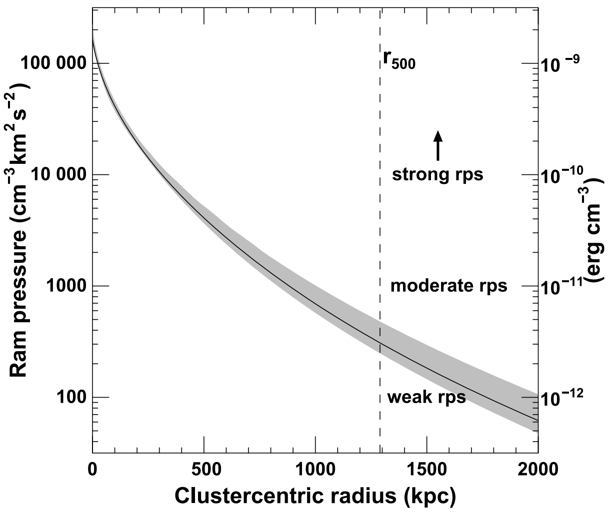

Figure 11. Effective ram-pressure ($\rho_{\rm ICM} v_{\rm orb}^2$) acting on galaxies infalling into Abell 3558 as a function of clustercentric radius (solid line), based on the gas/mass density profiles estimated by Sanderson & Ponman (2010) from *Chandra* X-ray data. The shaded regions indicate the 1σ errors extrapolated from the uncertainties in the Ascasibar & Diego (2008) model parameters obtained from 200 bootstrap resamplings of the original X-ray data (for details, see Sanderson & Ponman 2010).

dust/gas from the vicinity of the source of heating (the stars). Cortese et al. (2010b) found extraplanar cold dust in the perturbed galaxy NGC 4438 in Virgo collocated with the stripped atomic and molecular hydrogen. This extra-planar dust lacks a warm component or associated SF, leading to unusual f_{70}/f_{24} colours similar to those presented by our 70-μm-excess galaxies.

Finally, we check to see if ram-pressure stripping should be effective for these galaxies. For Abell 3558, Sanderson & Ponman (2010) derived the dark matter density, gas density ($\rho_{\rm ICM}$) and gas temperature profiles by fitting Ascasibar & Diego (2008) models to the *Chandra* X-ray data. In these models, the dark matter is described by a Hernquist (1990) density profile, which provides simple analytic expressions for the mass profile, gravitational potential and escape velocity ($v_{\rm esc}$). From this, we can derive the ram-pressure, $P_{\rm ram} = \rho_{\rm ICM} v_{\rm orb}^2$, acting on galaxies as a function of clustercentric radius, as shown in Fig. 11. For the orbital velocities, we assume the galaxies start at rest at the turnaround radius ($r_{\rm ta} \sim 3.5 r_{200}$) and fall radially. We find values of $\sim$1000 cm^{-3}(km s^{-1})^2 at 0.68r_{500} (where r_{500} = 1.29 Mpc; Sanderson, O'Sullivan & Ponman 2009), indicative of moderate ram-pressure stripping, capable of partially stripping an L^* spiral with rotational velocity $v_{\rm rot} \sim$ 150–200 km s^{-1} (e.g. Vollmer et al. 2001; Roediger & Hensler 2005; Kronberger et al. 2008), rising to ram-pressures of $\sim$10 000 cm^{-3}(km s^{-1})^2 at 0.24r_{500}, at which point all of the gas may be rapidly stripped from such galaxies. Thus for the bulk of our 70-μm-excess galaxies, which lie within $\sim$0.5–1.0 r_{500}, moderate to strong ram-pressure stripping should be effective.

Furthermore, the velocity dispersion of the 13 70-μm-excess galaxies within r_{500} of Abell 3558 is 948 km s^{-1}, marginally lower than the 975 $\pm$ 39 km s^{-1} obtained for the global cluster population within r_{500}. This would indicate that these 70-μm-excess galaxies are a virialized population, having been embedded in the dense intracluster medium (ICM) for a Gyr or more, rather than being on their first infall into the cluster. The fact that they make up 8 $\pm$ 2 per cent of the cluster galaxy population would also imply that this 70-μm-excess phase is long-lived, rather than the rapid evolution typically expected from ram-pressure stripping of infalling spirals, but, as Young et al. (2011) argue, the molecular gas content should be much more resistant to ram-pressure stripping than the easily removed H I component.

4.2 Morphological quenching

The 70-μm-excess galaxies are morphologically identified as S0s, with smooth profiles and absent spiral arms. An alternative mechanism that could cause the decline in SF to occur more rapidly than the reduction in the dust/gas content could be morphological quenching. In this hypothesis, recently developed by Martig et al. (2009), the morphological transformation from spiral to lenticular makes the gas (and collocated dust) more stable against fragmentation and collapse into molecular clouds, leading to a quenching of SF for a constant gas/dust fraction. The 24-μm flux tracing the SF continues to decline, while the 70-μm flux comes predominately from the cold interstellar dust content. The general ISRF in the bulge is predicted to be sufficiently strong to heat this dust without requiring young stars due to the high central density of stars (Jura 1982). *IRAS* detected FIR emission from a large fraction of nearby early-type galaxies, showing that they contained diffuse cool interstellar matter (Knapp et al. 1989; Goudfrooij & de Jong 1995; Merluzzi 1998). Recent *Herschel* observations of nearby galaxies by Engelbracht et al. (2010) and Bendo et al. (2010) show that the temperatures of the cool dust component in the central regions of early-type spirals (S0–Sb) are 20–50 per cent higher than in the discs, indicating that the dust is heated by the higher stellar density in the galactic bulge. Again this dust heating would be consistent with the SED fits of Rawle et al. (2010b) to their 100-μm-excess cluster population, although only one of their five 100-μm-excess galaxies with *Hubble Space Telescope* imaging appears bulge-dominated.

While early-type galaxies are classically defined as gas-poor passive systems, molecular gas, H I and warm dust was detected in 30 per cent of the SAURON representative sample of E/S0 galaxies (Combes, Young & Bureau 2007). Crocker et al. (2011) resolved the molecular gas for 12 SAURON galaxies into central discs or rings, coincident with the dust distribution (often in the form of tightly wound spiral structures) and corotating with the ionized gas. However, SF is the ionization source for just half of the sample, corresponding to those with the largest molecular gas reservoirs. Most of their E/S0s do not lie on the FIR–radio relation, having excess FIR flux, while the bolometric IR flux produces SFR estimates $\sim$3 times higher than those based on the 8- or 24-μm fluxes, due to additional heating from evolved stars in the bulge. Interestingly, one galaxy from their sample, NGC 4526 an S0 belonging to the Virgo cluster, is also a 70-μm-excess galaxy with $f_{70}/f_{24} \sim 30$, supporting the hypothesis that these are a cluster population. Of the 225 mostly field E/S0 galaxies in the *Spitzer*/MIPS study of Temi et al. (2009), only NGC 5866 and NGC 4526 have $f_{70}/f_{24} > 30$, again suggesting that this is a rare or short-lived phenomenon in isolated field E/S0s. The above results all reveal that a fraction of early-type galaxies have significant gas and dust contents, producing emission in the FIR, at levels above those predicted given their extremely low levels of SF.

4.3 Caveats with both scenarios

The presence of numerous S0s within the star-forming sequence of Fig. 1 and all along the quenching sequence of Fig. 10 appears to point towards a morphological scenario in which spirals are first transformed into S0s without necessarily affecting their SF, before being quenched morphologically. This however, does not explain why these transition dusty S0s with little or no SF are located almost exclusively in the dense cluster cores and appear so rare in isolated field regions. In contrast, the ram-pressure stripping scenario is able naturally to explain their concentration in the cluster cores where the dense ICM and high infall velocities make ram-pressure stripping most efficient. It does not however explain why these galaxies have already been morphologically transformed from spirals to S0s, as ram-pressure stripping is not predicted to strongly affect a galaxy's morphology. Instead, we would expect to find large numbers of spirals with little or no SF, which judging by Fig. 10 is not the case. However, we note that galaxies for which SF has been largely or completely quenched would not likely be detected at 70 μm and hence are not included in the figure.

4.4 Relating the quenching of SF to the morphological transformation of galaxies within clusters

To accurately account for the quenched galaxy population, and to be able to determine if indeed SF is primarily quenched *after* morphological transformation rather than before, we show in Fig. 12 the IR colour f_{24}/f_K versus K-band magnitude of confirmed Shapley supercluster galaxies, colour-coded according to their morphological classifications, allowing us to directly relate the bimodality in the SF activity to morphology. As we would expect, the passive galaxies ($f_{24}/f_K < 0.15$) are predominately early-types (E, E/S0, S0), while the normal star-forming galaxies ($f_{24}/f_K > 1.0$) are mostly spirals (Sa or later). There are however notable populations of both passive spirals and star-forming S0s.

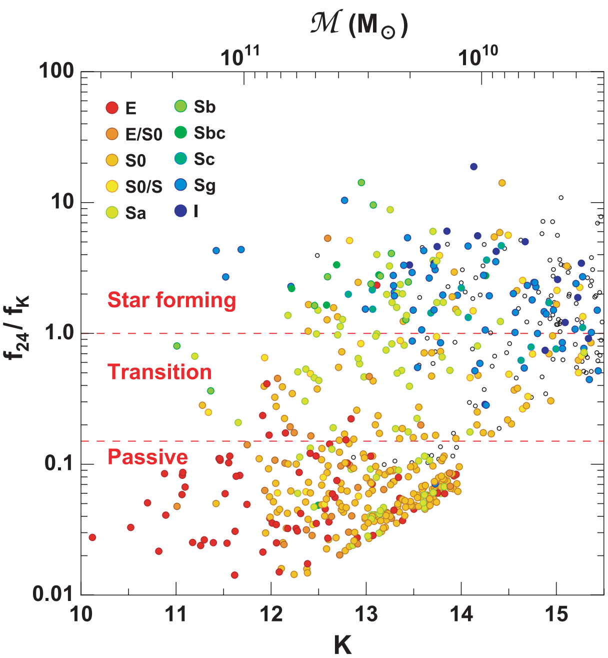

Figure 12. The IR colour f_{24}/f_K versus K-band magnitude for confirmed Shapley supercluster galaxies, colour-coded according to their morphologies indicated. The red dashed lines indicate how we separate galaxies into star-forming, transition and passive populations according the their f_{24}/f_K ratio as discussed in the text. Those galaxies not detected at 24 μm are also plotted, after being given a random 24-μm flux in the range 100–200 μJy, that is a factor 2–4 below the survey limit, and appear along the diagonal sequence passing through $K \sim 13.5$, $f_{24}/f_K \sim 0.05$.

Looking first at the 277 passive galaxies with $K < 14$, we find that $10.1^{+2.1}_{-1.5}$ per cent are classified as spirals (27 Sa, one Sg). These examples of massive spirals with low SFRs are reminiscent of the classic 'anemic spiral' of Van den Bergh (1976), although all show also a prominent bulge. This would be consistent with Bell (2008) who show that truly quenched central galaxies (i.e. most massive galaxies within their host dark matter halo) have stellar bulges, indicating that a bulge is an absolute requirement for full quenching of SF (at least in central galaxies). For these passive spirals, certainly ram-pressure stripping is a suitable candidate for removing their gas and quenching SF, in a manner similar to those spirals with truncated Hα discs and/or H I tails found in Virgo (Koopmann & Kenney 2004; Vogt et al. 2004; Crowl & Kenney 2008; Chung et al. 2009). Conversely, considering the 77 $K < 14$ star-forming galaxies, $18.2^{+5.2}_{-3.6}$ per cent are classified as early types (two S0/S, 10 S0, one E/S0, one E), for which it seems the morphological transformation has occurred *prior* to any significant quenching of SF. This time sequence is the opposite of what has been suggested by previous studies (e.g. Balogh et al. 2000; Bamford et al. 2009) which typically use optical colour as a proxy for SF activity. However, using *Spitzer* MIR data Wolf et al. (2009) revealed that these optically passive spirals still had significant obscured SF, albeit at levels 0.6 dex lower on average than normal star-forming galaxies of the same mass. They suggested that these apparent contradictions between the optical and MIR viewpoints reflected that the unobscured SF in the outer disc is the most susceptible to quenching by ram-pressure stripping, while the obscured component in the central parts remains relatively unaffected.

That there are comparable fractions and numbers of passive spirals and star-forming early-types indicates that SF in cluster galaxies is being quenched *both* before *and* after morphological transformation from spiral to S0. This is confirmed if we look at the morphologies of the transition galaxies with $0.15 < (f_{24}/f_K) < 1.0$ likely to be in the process of having their SF quenched. Here we find that $41.9^{+5.9}_{-5.5}$ per cent of the 74 $K < 14$ transition galaxies are spirals (26 Sa, two Sb, three Sg), and $58.1^{+5.5}_{-5.9}$ per cent are early-types (29 S0, two S0-S, six E/S0, six E). Among this latter population, many have excess 70-μm emission, producing MIR colours inconsistent with those seen in the local field population or by model IR SEDs.

The concentration of these transitional S0s with excess 70-μm emission towards the cluster cores points towards ram-pressure stripping being as the mechanism quenching the SF in these galaxies. However, assuming the simple Gunn & Gott (1972) criterion, the high central stellar densities of these S0s should significantly reduce the ability of ram-pressure stripping to completely remove their gas, while at low redshifts stellar mass loss should be capable of replenishing the gas supply required to maintain observed low levels of SF. As the findings of Young et al. (2011) show, a significant fraction of S0s are able to retain their molecular gas for several Gyr within the dense ICM of the Virgo cluster. The apparent 'virialized' dynamical status of the 70-μm-excess population suggests that these have also resided within the ICM for some time, rather than observed on their first infall. If this is the case, then it seems plausible that these are the direct descendants of the dusty starburst and post-starburst $\sim L^*$ galaxies abundant in clusters at $z \sim 0.4$ (Poggianti et al. 1999; Dressler et al. 2009), but which appear rare in present-day clusters.

5 SUMMARY

We have presented an analysis of the MIR colours of 165 70-μm-detected spectroscopic members of the SSC at $z = 0.048$, using panoramic *Spitzer*/MIPS 24- and 70-μm data. While the bulk of galaxies show MIR colours typical of local star-forming galaxies, we identified a significant population of 23 ‘70-μm-excess’ galaxies, comprising 14 ± 3 per cent of 70-μm-detected SSC galaxies whose MIR colours ($f_{70}/f_{24} > 25$) are much cooler than can be reproduced by any of the standard IR SED models. We examined in detail the nature of these galaxies, finding the following.

(i) They are strongly concentrated towards the cores ($\lesssim 0.5 r_{500}$) of the five clusters that make up the SSC, and also appear extremely rare among local field galaxies from the SINGS and SWIRE surveys, confirming them as a cluster-specific phenomenon.

(ii) Their intermediate f_{24}/f_K ratios place them in transition zone in which galaxies in the process of having their SF quenched are likely to be located.

(iii) Their optical spectra and lack of significant UV emission imply little or no ongoing SF.

(iv) They are primarily massive $\sim L_K^*$ galaxies with E/S0 morphologies, as confirmed by subsequent bulge–disc decompositions requiring comparable bulge and disc components to fit their *R*-band surface brightness profiles.

(v) Fits to their panchromatic SEDs require their FIR emission to be produced mostly by the diffuse dust component heated by the general ISRF rather than the clumpy component related to ongoing SF. Given that for most of these galaxies there is no evidence of ongoing or recent SF, the origin of this dust heating mechanism remains unclear.

The joint analyses of the IR colours and morphologies reveal that a primary evolutionary pathway for the formation of passive S0s in cluster cores involves the *prior* morphological transformation of spirals into S0s, perhaps via pre-processing or the impact of cluster tidal fields, before a subsequent quenching of SF once the S0 encounters the dense environment of the cluster core. Many of the cluster S0s in this latter stage of transformation, that is in the process of having their SF quenched, are characterized by excess 70-μm emission, indicating that their cold dust contents are probably declining at a slower rate than their SF. This observation, their concentration within the cluster cores, and their apparent virialized dynamical status draw strong parallels with the population of molecular gas-rich S0s identified by Young et al. (2011) in the Virgo cluster. These results suggest then that S0s are able to retain both their molecular gas and dust contents for a significant length of time ($\gtrsim$1 Gyr) within the ICM, after being accreted by a cluster. These thus represent a key transition population that can be used to understand the physical mechanisms behind the formation of many passive lenticulars in local clusters.

We put forward two possible causes for these cluster S0s with excess 70-μm emission: (i) assuming the dust-to-gas ratio remains constant, the 70-μm excess suggests a reduction in the SF efficiency in these dusty cluster S0s as proposed within the morphological quenching scenario or (ii) a 2–3 times increase in the dust-to-gas ratio or metallicity of the remnant ISM of these galaxies, as predicted by multizone chemical evolutionary models of galaxies in the process of being ram-pressure stripped or starved. In this latter scenario, the accretion of pristine gas is shut down, and so no longer dilutes the remaining H I gas enriched by metals recycled by stellar mass loss.

This evolutionary pathway is quite different from the often considered view that SF is quenched in spiral galaxies once they encounter the cluster environment, forming the classic anemic spiral population (Van den Bergh 1976; Poggianti et al. 1999; Balogh et al. 2000), which are then transformed somehow into lenticulars. Notably, we identify significant populations of both star-forming S0s and passive spirals which reveal that SF in cluster galaxies is being quenched both *before* and *after* morphological transformation from spiral to lenticular, and that both pathways are of comparable relevance. This was confirmed when we looked at the transition galaxies likely to be in the process of having their SF quenched, finding them to made up of 42 per cent spirals (mostly Sa) and 58 per cent early-type galaxies, most of which were S0s.

These results confirm that the environmental processes behind the SFR–density and morphology–density relations are complex and are far from being fully understood. The availability of FIR data is allowing us now to probe directly the ISM via its dust content, which, given that the environmental processes behind the quenching of SF in cluster galaxies are likely to act directly on the ISM rather than the star-forming regions themselves, will be crucial in fully understanding the origin of the SF–density relation.

ACKNOWLEDGMENTS

The authors thank the referee A. Dressler for his constructive report and positive feedback regarding this work. This work was carried out in the framework of the collaboration of the FP7-PEOPLE-IRSES-2008 project ACCESS. CPH, RJS and GPS acknowledge financial support from STFC. GPS acknowledges support from the Royal Society. CPH, GB and PM thank Mike Dopita and the Australian National University for their hospitality. We thank Alastair Sanderson for providing the gas/mass density profiles and uncertainties for Abell 3558. CPH and GPS thank Tim Rawle, Eiichi Egami, Maria Pereira, Alessando Boselli and Samuel Bossier for useful discussions. This work is based in part on observations made with the *Spitzer Space Telescope*, which is operated by the Jet Propulsion Laboratory, California Institute of Technology under a contract with NASA.

REFERENCES

Abazajian K. N. et al., 2009, ApJS, 182, 543
Andrews B. H., Thompson T. A., 2011, ApJ, 727, 97
Ascasibar Y., Diego J. M., 2008, MNRAS, 383, 369
Balogh M. L., Navarro J. F., Morris S. L., 2000, ApJ, 540, 113
Balogh M. L., Couch W. J., Smail I., Bower R. G., Glazebrook K., 2002, MNRAS, 335, 10
Balogh M. L. et al., 2004, MNRAS, 348, 1355
Bamford S. P. et al., 2009, MNRAS, 393, 1324
Bell E. F., 2008, ApJ, 682, 355
Bendo G. J. et al., 2010, A&A, 518, L65
Boselli A., Gavazzi G., 2006, PASP, 118, 517
Boselli A., Boissier S., Cortese L., Gavazzi G., 2008, ApJ, 674, 472
Bressan A. et al., 2006, ApJ, 639, L55
Bretherton C. F., James P. A., Moss C., Whittle M., 2010, A&A, 524, 24
Bruzual G., Charlot S., 2003, MNRAS, 344, 1000
Byrd G., Valtonen M., 1990, ApJ, 350, 89
Calzetti D. et al., 2010, ApJ, 714, 1256
Christlein D., Zabludoff A. I., 2004, ApJ, 616, 192
Chung A., van Gorkom J. H., Kenney J. D. P., Crowl H., Vollmer B., 2009, AJ, 138, 1741
Coia D. et al., 2005, A&A, 431, 433
Combes F., Young L. M., Bureau M., 2007, MNRAS, 377, 1795
Compiègne M. et al., 2011, A&A, 525, 103

Cortese L. et al., 2010a, A&A, 518, L49
Cortese L. et al., 2010b, A&A, 518, L63
Couch W. J., Sharples R. M., 1987, MNRAS, 229, 423
Crocker A. F., Bureau M., Young L. M., Combes F., 2011, MNRAS, 410, 1197
Crowl H. H., Kenney J. D. P., 2008, AJ, 136, 1623
da Cunha E., Charlot S., Elbaz D., 2008, MNRAS, 388, 1595
da Cunha E., Eminian C., Charlot S., Blaizot J., 2010, MNRAS, 403, 1894
Dale D. A., Helou G., 2002, ApJ, 576, 159
Dale D. A., Helou G., Contursi A., Silbermann N. A., Kolhatkar S., 2001, ApJ, 549, 215
Davis T. A. et al., 2011, preprint (arXiv:1107.0002)
de Vaucouleurs G., 1959, Handbuch de Physik, 53, 275
de Vaucouleurs G., 1963, ApJS, 8, 31
Désert F.-X., Boulanger F., Puget J. L., 1990, A&A, 237, 215
Dib S., Piau L., Mohanty S., Braine J., 2011, preprint (arXiv:1102.3839)
Dopita M. A. et al., 2005, ApJ, 619, 755
Dopita M. A. et al., 2011, Ap&SS, 333, 225
Doyon R., Joseph R. D., 1989, MNRAS, 239, 347
Draine B. T. et al., 2007, ApJ, 663, 866
Dressler A., 1980, ApJ, 236, 351
Dressler A., Gunn J. E., 1983, ApJ, 270, 7
Dressler A., Thomson I. B., Schechtman S. A., 1985, ApJ, 288, 481
Dressler A. et al., 1997, ApJ, 490, 577
Dressler A., Rigby J., Oemler A., Jr, Fritz J., Poggianti B. M., Rieke G., Bai L., 2009, ApJ, 693, 140
Duc P.-A. et al., 2002, A&A, 382, 60
Engelbracht C. W. et al., 2010, A&A, 518, L56
Fadda D., Biviano A., Marleau F. R., Storrie-Lombardi L. J., Durret F., 2008, ApJ, 672, L9
Frayer D. T. et al., 2006, ApJ, 647, L9
Gargiulo A. et al., 2009, MNRAS, 397, 75
Geach J. E. et al., 2006, ApJ, 649, 661
Goudfrooij P., de Jong T., 1995, A&A, 298, 784
Groves B., 2004, PhD thesis, Australian National University
Groves B., Dopita M. A., Sutherland R. S., Kewley L. J., Fischera J., Leitherer C., Brandl B., van Breugel W., 2008, ApJS, 176, 438
Gunn J. E., Gott J. R., III, 1972, ApJ, 176, 1
Haines C. P., Merluzzi P., Mercurio A., Gargiulo A., Krusanova N., Busarello G., La Barbera F., Capaccioli M., 2006, MNRAS, 371, 55
Haines C. P., Gargiulo A., La Barbera F., Mercurio A., Merluzzi P., Busarello G., 2007, MNRAS, 381, 7
Haines C. P., Gargiulo A., Merluzzi P., 2008, MNRAS, 385, 1201
Haines C. P., Smith G. P., Egami E., Moran S. M., Sanderson A. J. R., Merluzzi P., Busarello R., Smith R. J., 2009, ApJ, 704, 126
Haines C. P., Smith G. P., Pereira M. J., Egami E., Moran S. M., Hardegree-Ullman E., Rawle T., Rex M., 2010, A&A, 518, L19
Haines C. P., Busarello G., Merluzzi P., Smith R. J., Raychaudhury S., Mercurio A., Smith G. P., 2011a, MNRAS, 412, 127 (Paper II)
Haines C. P., Busarello G., Merluzzi P., Smith R. J., Raychaudhury S., Mercurio A., Smith G. P., 2011b, MNRAS, 412, 145 (Paper III)
Hernquist L., 1990, ApJ, 356, 359
Jura M., 1982, ApJ, 254, 70
Katgert P. et al., 1996, A&A, 310, 8
Kennicutt R. C., Jr et al., 2003, PASP, 115, 928
Kewley L. J., Jansen R. A., Geller M. J., 2005, PASP, 117, 227
Knapp G. R., Guhathakurta P., Kim D.-W., Jura M. A., 1989, ApJS, 70, 329
Koopmann R. A., Kenney J. D. P., 2004, ApJ, 613, 866
Kramer C. et al., 2010, A&A, 518, L67
Kronberger T., Kapferer W., Ferrari C., Unterguggenberger S., Schindler S., 2008, A&A, 481, 337
La Barbera F., de Carvalho R. R., Kohl-Moreira J. L., Gal R. R., Soares-Santos M., Capaccioli M., Santos R., Sant'anna N., 2008, PASP, 120, 681
Leitherer C. et al., 1999, ApJS, 123, 3
Leitner S. N., Kravtsov A. V., 2011, ApJ, 734, 48
Leonardi A. J., Rose J. A., 1996, AJ, 111, 182
Li J.-T., Wang Q. D., Li Z., Chen Y., 2009, ApJ, 706, 693
Li Y., Calzetti D., Kennicutt R. C., Hong S., Engelbracht C. W., Dale D. A., Moustakas J., 2010, ApJ, 725, 677
Lonsdale Persson C., Helou G., 1987, ApJ, 314, 513
Lonsdale C. et al., 2003, PASP, 115, 897
Mahajan S., Haines C. P., Raychaudhury S., 2010, MNRAS, 404, 1745
Mahajan S., Haines C. P., Raychaudhury S., 2011, MNRAS, 412, 1098
Martig M., Bournard F., 2010, ApJ, 714, L275
Martig M., Bournard F., Teyssier R., Dekel A., 2009, ApJ, 707, 250
Mercurio A., Busarello G., Merluzzi P., La Barbera F., Girardi M., Haines C. P., 2004, A&A, 424, 79
Mercurio A. et al., 2006, MNRAS, 368, 109
Merluzzi P., 1998, A&A, 338, 807
Merluzzi P., Mercurio A., Haines C. P., Smith R. J., Busarello G., Lucey J. R., 2010, MNRAS, 402, 753 (Paper I)
Mihos J. C., Hernquist L., 1994, ApJ, 431, L9
Moran S. M., Miller N., Treu T., Ellis R. S., Smith G. P., 2007, ApJ, 659, 1138
Moss C., 2006, MNRAS, 373, 167
Neugebauer et al., 1984, ApJ, 278, L1
Peng C. Y., Ho L. C., Impey C. D., Rix H., 2002, AJ, 124, 266
Pereria M. J. et al., 2010, A&A, 518, L40
Pilbratt G. L. et al., 2010, A&A, 518, L1
Piovan L., Tantalo R., Chiosi C., 2003, A&A, 408, 559
Poggianti B. M., Wu H., 2000, ApJ, 529, 157
Poggianti B. M., Smail I., Dressler A., Couch W. J., Barger A. J., Butcher H., Ellis R. S., Demler A. Jr, 1999, ApJ, 518, 576
Popescu C. C., Tuffs R. J., Völk H. J., Pierini D., Madore B. F., 2002, ApJ, 567, 221
Popescu C. C., Tuffs R. J., Dopita M. A., Fischera J., Kylafis N. D., Madore B. F., 2011, A&A, 527, 109
Rawle T., Smith R. J., Lucey J. R., 2010a, MNRAS, 401, 852
Rawle T. et al., 2010b, A&A, 518, L14
Raychaudhury S., 1989, Nat, 342, 251
Rieke G. H., Alonso-Herrero A., Weiner B. J., Pérez-Gonzélez P. G., Blaylock M., Donley J. L., Marcillac D., 2009, ApJ, 692, 556
Roediger E., Hensler G., 2005, A&A, 433, 875
Saintonge A. et al., 2011, MNRAS, 415, 61
Sanderson A. J. R., Ponman T. J., 2010, MNRAS, 402, 65
Sanderson A. J. R., O'Sullivan E., Ponman T. J., 2009, MNRAS, 395, 764
Sauvage M., Thuan T. X., 1992, ApJ, 396, L69
Shapiro K. L. et al., 2010, MNRAS, 402, 2140
Skillman E. D., Kennicutt R. C., Jr, Shields G. A., Zaritsky D., 1996, ApJ, 462, 147
Smail I., Morrison G., Gray M. E., Owen F. N., Ivison R. J., Kneib J. P., Ellis R. S., 1999, ApJ, 525, 609
Smith G. P., Treu T., Ellis R. S., Moran S. M., Dressler A., 2005, ApJ, 620, 78
Smith R. J., Lucey J. R., Hudson M. J., 2007, MNRAS, 381, 1035
Smith G. P. et al., 2010, A&A, 518, L18
Temi P., Brighenti F., Mathews W. G., 2009, MNRAS, 707, 890
Thomas T., Katgert P., 2006, A&A, 446, 19
Treu T., Ellis R. S., Kneib J.-P., Dressler A., Smail I., Czoske O., Oemler A., Natarajan P., 2003, ApJ, 591, 53
van den Bergh S., 1976, ApJ, 206, 883
Vazdekis A., Sánchez-Blázquez P., Falcón-Barroso J., Cennar A. J., Beasley M. A., Cardiel N., Gorgas J., Peletier R. F., 2010, MNRAS, 404, 1639
Vogt N. P., Haynes M. P., Giovanelli R., Herter T., 2004, AJ, 127, 3300
Vollmer B., Cayatte V., Balkowski C., Duschl W. J., 2001, ApJ, 561, 708
Wolf C., Gray M. E., Meisenheimer K., 2005, A&A, 443, 435
Wolf C. et al., 2009, MNRAS, 393, 1302
Young L. M. et al., 2011, MNRAS, 414, 940

This paper has been typeset from a TEX/LATEX file prepared by the author.